EXPERIMENTAL

EXPERIMENTAL SETUP-DESCRIPTION

The schematic diagram of the experimental setup for the 6" column is depicted in Fig. 1. The bubble column is constructed of plexiglas and its inside diameter is 0.1524m(6") with a wall thickness of 0.0127m(1/2"). The total height of the column is 5.32m, consisting of four 1.33m sections flanged together. The gas distribution system occupies 0.1524m of the column, making the effective height of the column equal to 5.16m. A total of eleven pressure taps are in the column, the lowest being 0.1016m(4") above the distributor. The distances between the bottom five taps is 0.3048(12") and the remaining pressure taps are 0.6096m(24") apart. This enables the study of local holdup. The pressure taps have been drilled with great care to reduce possible velocity head effects. A 0.8mm(1/32") hole has been drilled in the column wall and the inner surface polished to remove any burrs (eliminate velocity and friction head effects). The tappings are all connected to a manometer board by means of flexible polypropylene tubing. The manometric board consists of 10 U-tube manometers filled with carbon tetrachloride as the manometric fluid. The connecting lines are filled with the column liquid.

Air is supplied by an existing compressor through a pressure regulator, air filter, rotameter, and a control valve to regulate the gas flow rate. Tap water is pumped from a 0.3785m (100 gallon) tank, through a water filter, control valve and a rotameter. Air enters the column at the bottom, through the gas distributing region. Three different positions for the liquid entrance directly to the column are located 0.0508m(2"), 0.06096(24") and 1.371m(54") above the distributor plate. The air-water mixture flows up the column, and then into a gas-liquid

separation tank, where the air is vented and the water recirculated back to the storage tank. Quick closing ball valves are attached to the entrance (both air and water) of the column. The air rotameter has been calibrated using an air flow meter, while the water rotameter has been calibrated by collecting the water in a tank for a specific time and measuring its volume.

The gas distribution system, consists of a conical section packed with 3.5mm borosilicate glass beads, and a 0.127m(5") diameter distributor plate placed on top. The distributor plate is fitted, so as to make sure air enters only through the distributor plate, and not through the side of the plate. Air entering from the sides, usually in the form of big bubbles, disrupts the flow pattern, especially in the case of uniform bubbling.

The schematic diagram of a 0.33 meter inside diameter and 5.32m high bubble column is shown in Fig. 2. Air was supplied by a ten horsepower compressor and was filtered and regulated prior to its introduction to the bottom of the column. Two rotameters were utilized to measure a large variety of air flow. Temperature and pressure of the air were also measured to correct the velocities to the column conditions. Liquid was introduced to the column at a point just above the distributor plate and was supplied by a one horsepower pump. Liquid velocities were measured using a bypass rotameter arrangement calibrated for each fluid. Liquid was stored in and recirculated through a 170 gallon tank. Another tank was used for solution makeup. The air-liquid mixture leaving the column was separated by overflowing into a trough, the air being released to the atmosphere and the liquid draining back into the 170 gallon tank.

HOLDUP MEASUREMENT

Two methods were employed to measure gas holdup. Static pressure drop was used to measure local axial holdup at intervals along the column. A manometer containing carbon tetra chloride was used to measure the static pressure. This method measures the bulk density of the two phase mixture by means of an energy balance around the manometer and the section of the column being measured. The bulk density of the two phase mixture is related to the gas holdup as follows:

$$E_G = 1 - \rho_m/\rho_w$$

This equation ignores the density of the gas which may be neglected under the test conditions.

The other method used to measure gas holdup was by measuring bed expansion. In this method the height of the two phase mixture was measured then the air and liquid flows were stopped simultaneously, the liquid height in the column was then measured after all the air had escaped. Holdup by this method can then be determined as follows:

$$E_G = (h_1-h_2)/(h_T-h_1)$$

FLOW PATTERN DETERMINATION

Flow patterns and transition regions between patterns were determined through visual observation. Photographic methods were utilized to enhance observations. The bubble to bubble slug transition region was also determined by observing the holdup versus gas velocity data. In using this method the maximum and minimum holdup on the holdup versus velocity curve using a porous plate distributor indicated the boundaries

of the transition zones.

NON-NEWTONIAN FLUIDS

Eight different non-Newtonian fluids were studied (see Table 1). These include four carboxymethyl cellulose (CMC) solutions and four CMC and isopropyl alcohol (IPA) solutions. CMC was chosen for its pseudoplastic behavior, its popularity for use in researching non-Newtonian fluids, its stability under shear and its non-harzardous nature, (26).

The rheology of CMC solutions is pseudoplastic and can be characterized using the power model, i.e.:

$$\tau_{yx} = k(\dot{\gamma})^{n-1}\dot{\gamma}$$

Solutions containing IPA were utilized to provide a variation in surface tension.

Flow curves and power law coefficients were determined using a Haake RV-12 viscometer. Surface tension was measured using a Dougnoy-ring tensiometer.

GAS DISTRIBUTORS

Eighteen different porous plates were used to study the effect of porous plates on gas holdup and flow pattern in a bubble column. The details of the distributor plates are given in Table 2. The effect of pore size, plate material and wettability were studied.

FLUID VELOCITIES

Gas velocities were varied for each run between 0.003 and 0.012m/s. This range of gas velocities were studied to provide measurements well into the bubble-slug flow pattern (see Figure 3). The number of velocities studied within this range varied between eight and ten depending on the fluid.

Three liquid velocities were studied for each fluid; 0, 0.005 and 0.012m/s. For each fluid and distributor plate runs were repeated for each of these liquid velocities.

BUBBLE SIZES

Bubble sizes were determined for each fluid and distributor plate as a function of gas velocity. Still picture photography was utilized to measure bubble sizes. A transparent millimeter scale was included in all photographs to facilitate measurement of bubble diameters.

Sauter average bubble diameters were determined for each photography. The sauter average was calculated from:

$$d_{SB} = \frac{nd_B^3}{nd_B^2}$$

EXPERIMENTAL PROCEDURE

Gas holdup experiments were conducted at three different liquid velocities and then two types of distributor plates. Table 1 lists the solute concentrations and liquid velocities for each distributor plate and experimental run.

The procedure used in these experiments was as follows:

1. the column was filled with liquid.

2. The gas shutoff valve was actuated and the velocity was adjusted to one of the predetermined meter calibrations.
3. The differential pressure between the top two presure taps on the column were monitored.
4. The gas velocity was monitored and adjusted as needed.
5. The liquid velocity was monitored and adjusted as needed.
6. When the pressure differential at the top of the column became constant, usually after five minutes but as long as twenty, the gas meter reading, gas temperature, and pressure were recorded.
7. The differential pressure between all of the pressure taps, beginning at the top of the column. Each time the manometer valves were switched the new differential pressure was monitored until a new equilibrium condition was established.
8. Finally the height of the two-phase mixture in the column was measured if the liquid velocity was zero. If the liquid velocity was not zero the bed height was considered the top of the column. The electric shutoff valves were then actuated, first the liquid then the gas. The height of the liquid was then measured after the gas had left the bed.
9. Observations were made during each run concerning bubble sizes and flow patterns. These observations were recorded on the respective runs data sheets.

SOLUTION MAKEUP

Different solutions were utilized in the experiments; water, IPA and CMC solutions and CMC solutions without IPA. Only one concentration of IPA (eight percent by weight) was used in solutions that contained IPA. The solutions, their concentrations and physical properties are detailed

in Table 3.

The solution makeup procedure was as follows:

1. The small tank was filled to three quarters with deionized water and the large tank was filled to one hundred gallons with deionized water.
2. CMC was added to the small tank by slowly shaking the CMC in the proximity of the agitator. The agitator speed was adjusted as CMC was added to maintain a high circulation rate.
3. If IPA was used, it was added to the one hundred gallons of water in the large tank.
4. When the CMC in the small tank had dissolved, usually after two hours or when the solution became clear, it was pumped into the large tank. The solution in the large tank was then pumped back into the small tank several times to rinse the small tank.
5. Finally, the small tank was rinsed with deionized water several times, pumping the rinse water into the large tank. The large tank was then filled to the one hundred seventy gallon mark.

PHOTOGRAPHIC PROCEDURE

The borescope was set inside the column at 141 cm above the distributor and 2.5cm from the wall and approximately 18 pictures taken with the focus distance set 2mm from the tip of the borescope. Photographs were also taken with the borescope located at 5cm, 7.5cm, 12.5cm and in the center line of the column. In earlier experiments, the borescope was switched to the lowest axial position to see the variation in the bubble sizes. Photographs of a ruler with 0.5mm divisions were taken at the same focal distance as that set in the borescope in order to have a pattern of comparison for the bubble sizes.

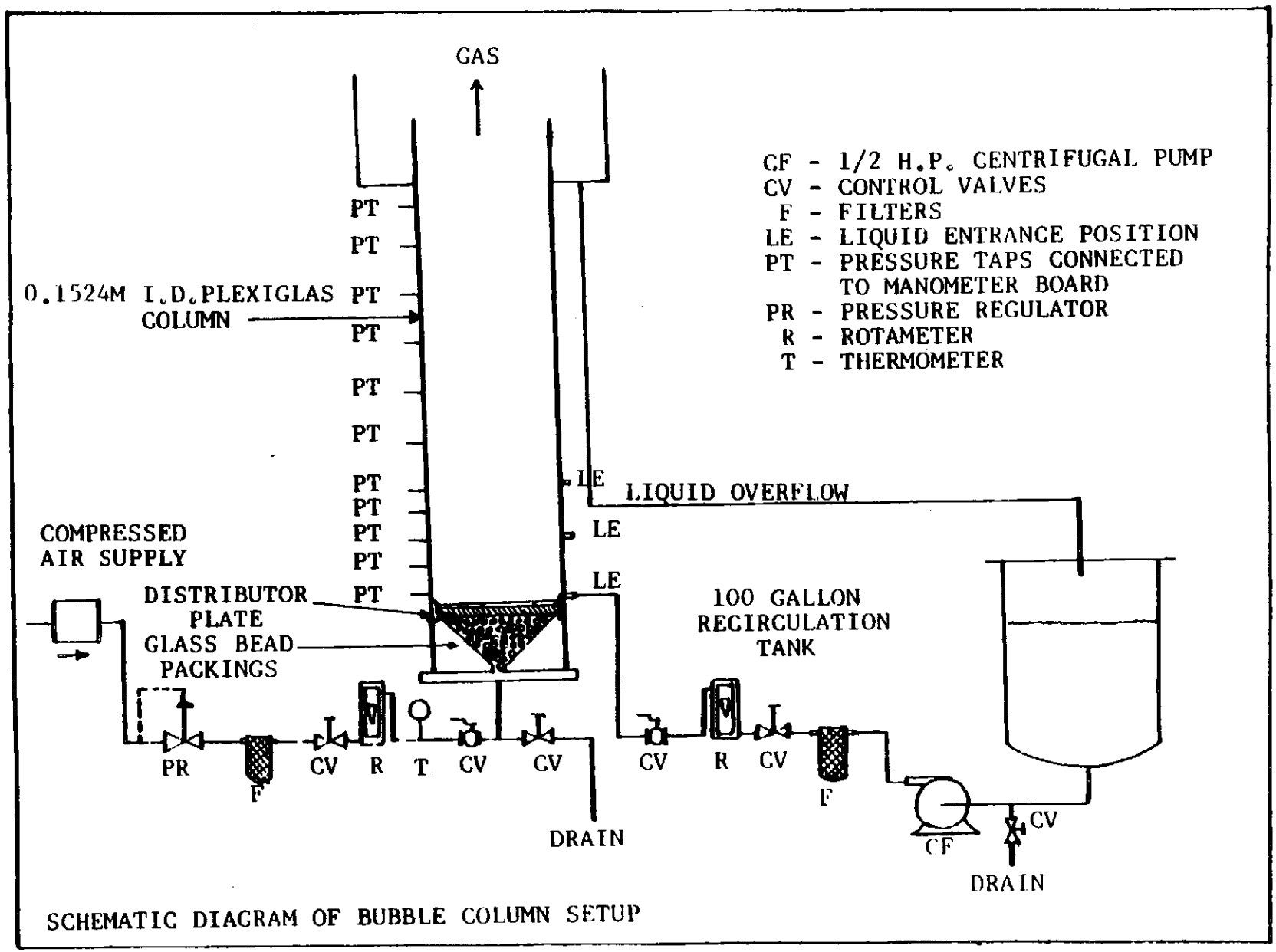

SCHEMATIC DIAGRAM OF BUBBLE COLUMN SETUP

FIGURE 1

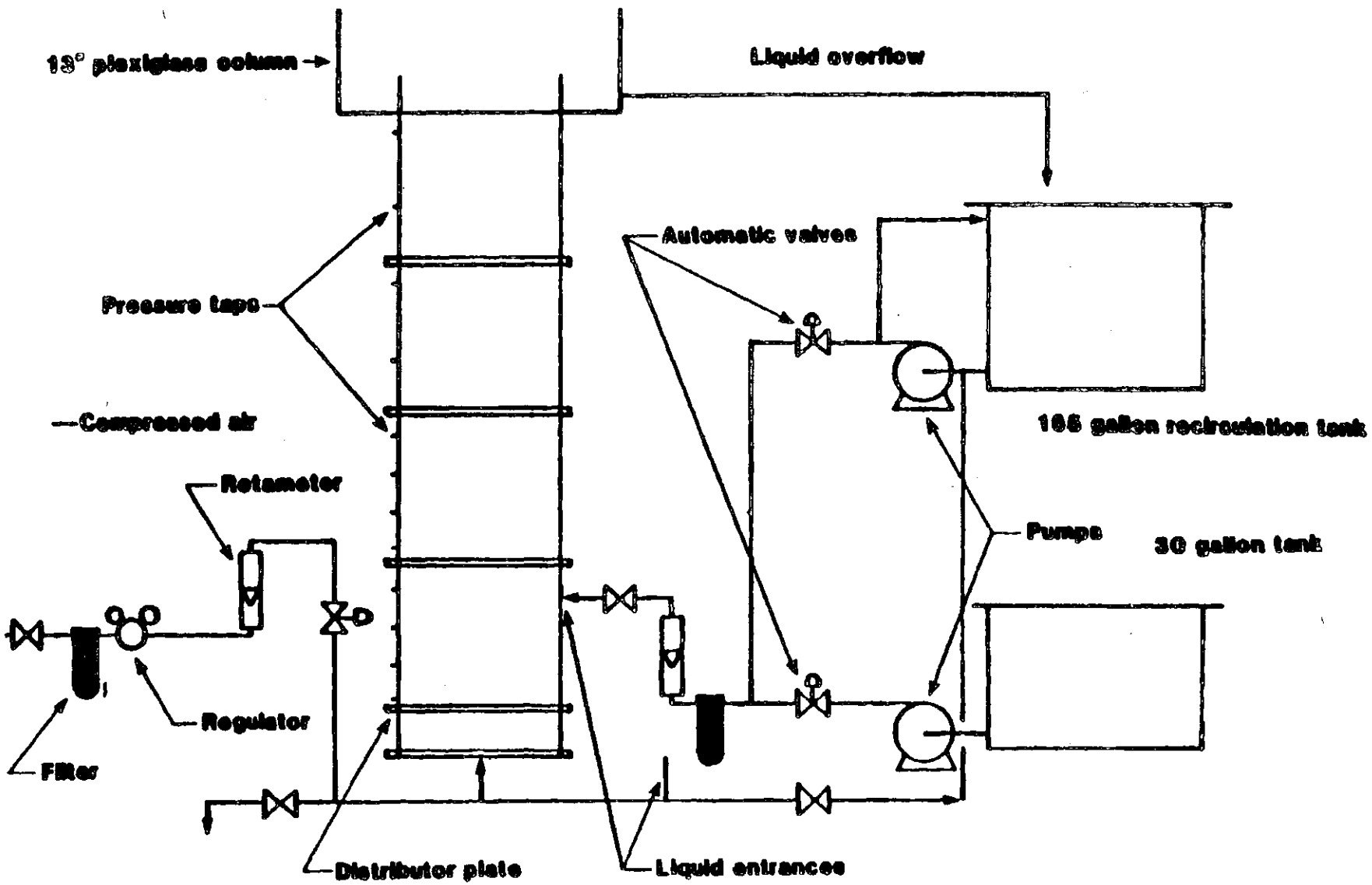
19° plexiglass column
Liquid overflow
Automatic valves
Pressure taps
Compressed air
Rotameter
105 gallon recirculation tank
Pumps
30 gallon tank
Regulator
Filter
Distributor plate
Liquid entrances

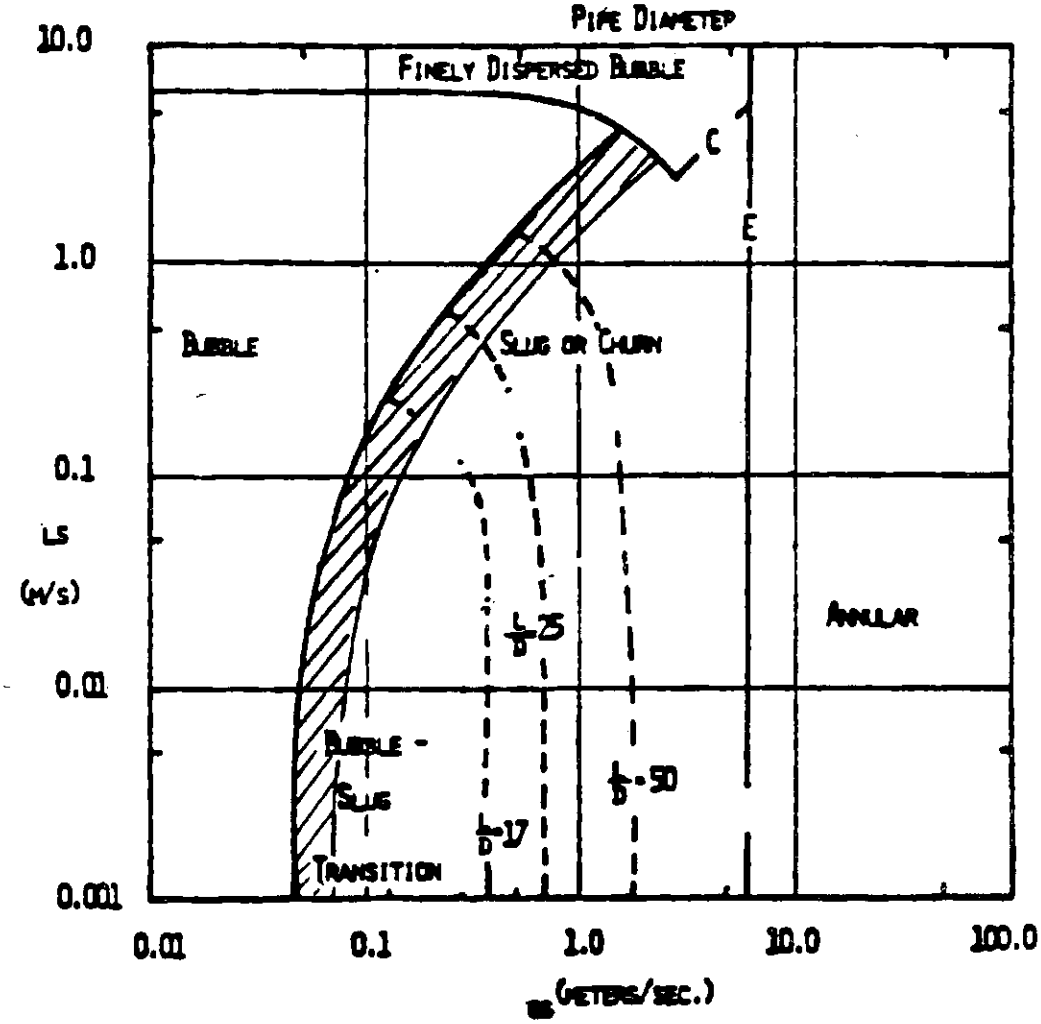

Figure 3 Flow Map for the Air-Water System

TABLE 1 EXPERIMENTAL RUNS USING AQUEOUS CMC SOLUTION

POROUS PLATE				SIEVE PLATE			
RUN#	CMC CONC. (wt. %)	IPA CONC. (wt. %)	LIQUID VEL. (M/S)	RUN#	CMC CONC. (wt. %)	IPA CONC. (wt. %)	LIQUID VEL. (M/S)
2	0.0	0.0	0.0	1	0.0	0.0	0.0
3	0.5	8.0	0.0	6	0.5	8.0	0.0
4	0.5	8.0	0.005	7	0.5	8.0	0.005
5	0.5	8.0	0.012	8	0.5	8.0	0.012
12	0.25	8.0	0.0	9	0.25	8.0	0.0
13	0.25	8.0	0.012	10	0.25	8.0	0.005
14	0.25	8.0	0.005	11	0.25	8.0	0.012
18	1.0	8.0	0.0	15	1.0	8.0	0.0
19	1.0	8.0	0.005	16	1.0	8.0	0.005
20	1.0	8.0	0.012	17	1.0	8.0	0.012
21	0.75	8.0	0.0	23	0.75	8.0	0.012
22	0.75	8.0	0.005	24	0.75	8.0	0.0
29	0.25	0.0	0.0	25	0.75	8.0	0.005
30	0.25	0.0	0.005	26	0.25	0.0	0.0
31	0.25	0.0	0.012	27	0.25	0.0	0.005
32	0.5	0.0	0.0	28	0.25	0.0	0.012
33	0.5	0.0	0.005	35	0.5	0.0	0.0
34	0.5	0.0	0.012	36	0.5	0.0	0.005
41	0.75	0.0	0.0	37	0.5	0.0	0.012
42	0.75	0.0	0.005	38	0.75	0.0	0.0
43	0.75	0.0	0.012	39	0.75	0.0	0.005
44	1.0	0.0	0.0	40	0.75	0.0	0.012
45	1.0	0.0	0.005	47	1.0	0.0	0.0
46	1.0	0.0	0.012	48	1.0	0.0	0.005
50	0.75	0.0	0.0	49	1.0	0.0	0.012
51	0.75	0.0	0.005	53	0.0	8.0	0.0
52	0.75	0.0	0.012	54	0.0	8.0	0.005
56	0.0	8.0	0.0	55	0.0	8.0	0.012
57	0.0	8.0	0.005				
58	0.0	8.0	0.012				

TABLE NO. 2

POROUS PLATE GAS DISTRIBUTOR DETAILS

KEY	PORE SIZE (μ)	THICKNESS (M)	MATERIAL	CHARACTERISTICS
PEL 1	35	0.00635	Polyethylene	Hydrophilic
PEL 2	35	0.0127	Polyethylene	Hydrophilic
PEL 3	70	0.00159	Polyethylene	Hydrophilic
PEL 4	70	0.00317	Polyethylene	Hydrophilic
PEL 5	70	0.00635	Polyethylene	Hydrophilic
PEL 6	70	0.0127	Polyethylene	Hydrophilic
PEB 1	70	0.00159	Polyethylene	Hydrophobic
PEB 2	70	0.00317	Polyethylene	Hydrophobic
PEB 3	70	0.00635	Polyethylene	Hydrophobic
PEB 4	70	0.0127	Polyethylene	Hydrophobic
PPL 1	125	0.00635	Polypropylene	Hydrophilic
PPL 2	125	0.0127	Polypropylene	Hydrophilic
SC 1		0.00317	Silicon Carbide	
SC 2		0.00635	Silicon Carbide	
AO 1		0.0254	Aluminum Oxide	Porosity 34-38%
AO 3	240	0.0254	Fused Alumina Grains	Permeability 50 Cfm/cu.ft
PP			Plastic Porous	
SE				
SE Hole Diameter 0.00317m		0.00317	Plexiglas	Traingular Pitch = 0.009525m

Table 3 Liquid Physical Properties

CMC Conc. (wt. %)	IPA Conc. (wt. %)	Specific Gravity	Surface Tension (Dynes/ CM)	Power Law Parameters K	N
0.0	0.0	1.0	72	0.01	1.0
0.25	0.0	1.0	72	0.012	0.97
0.5	0.0	1.0	72	0.015	0.95
0.75	0.0	1.0	72	0.025	0.91
1.0	0.0	1.0	72	0.04	0.88
0.0	8.0	0.986	45	0.009	1.0
0.25	8.0	0.986	45	0.018	0.958
0.5	8.0	0.986	45	0.034	0.918
0.75	8.0	0.986	45	0.06	0.878
1.0	8.0	0.986	45	0.095	0.833

RESULTS

Holdup studies were made on different porous plate gas distributors and different CMC solutions.

Holdup showed a maximum with superficial gas velocity for all the porous plate distributors. This maximum is shifted to lower gas velocities as CMC concentration is increased. However, for high CMC concentrations this maximum was obtained at the superficial gas velocity of 1 cm/s. Also, the maximum in holdup tends to vanish with increasing CMC concentration.

Holdup decreased sharply at a certain value of VGS which is the transition value from bubble to bubble-slug flow. The decrease in the gas holdup at the transition was due to the coalescence of bubbles. The transition occurred above superficial gas velocity ranging from 0.054 m/s to 0.085 m/s for different porous plates. The gas holdup at this transition varied from 0.2 to 0.33 for different porous plate gas distributors. Bubble-slug to churn-slug transition occurred at superficial gas velocity of about 0.22 m/s. Using sieve plate distributors, the holdup was significantly lower than with porous plates as seen in Figure 1. The transition region that was observed in porous plates was not observed when using sieve plate distributors.

The bubble to bubble-slug flow transition was observed for all of the fluids studied. This transition varied with both CMC and IPA concentrations. Transitions were only observed visually. However, in some CMC-IPA solutions the change was so subtle, the point where bubble slug flow began could not be pinpointed. This was the case with two of the CMC-IPA solutions, 0.25% CMC and 0.5% CMC. In these solutions a gradual appearance of substantially larger bubbles (20mm as opposed to 1-5mm) with increasing gas velocity occurred. But the point which the

flow pattern changed was not obvious. The IPA solution with 0.75%wt CMC showed a well defined transition from bubble to bubble-slug while the IPA solution showed a dependence on height in the column. Coalescence began at the top of the column and moved downward with increased gas velocity. The behavior above and below the transition point in the column was easy to distinguish. The two phase mixture at the top was highly turbulent and very large bubbles occurred with a short frequency. The mixture at the bottom of the column displayed a lot of backmixing but not the violent action observed at the top and no very large bubbles were observed in the bottom.

The holdup for different CMC concentrations at the same gas velocity is always lower for the higher polymer concentration in the bubble-slug pattern.

A phenomenon that hampered observation of flow pattern transition in the IPA solutions was the occurrence of foam in the column. In the bubble flow pattern foaming was extensive and with no liquid flow the foam was observed to overflow the column for as long as twenty minutes. Once the transition point was past, the foam broke down however.

The pore size was varied from 35 to 70 microns and the data was plotted in Fig. 2. Holdup increased with an increase in pore size in the bubble, and the bubble-slug flow patterns. The increase in holdup was about 15% in the bubble flow pattern and about 8% in the bubble slug flow pattern. There was no variation in holdup in the churn-slug flow pattern ($< 5\%$, i.e., within experimental error). Holdup at the transition varied with pore size with a maximum deviation of 25%.

Aoyama et al (5) used a 0.05m diameter column and 0.003m thick porous plate distributor and found that the transition occurring at 0.06 m/s and holdup of 0.27 for tap water. In the present work the thickness of the

plates varied from 0.016m (1/16") to 0.0127m (1/2"). Holdup increased with increase in the distributor thickness, the effect being more in the bubble flow pattern. Distributor plate with 0.0127m thickness gave errors in the holdup measurements. Two 0.00635m plates were fixed together to give 0.0127m thickness and there were leakages from the side of the distributor. This gave errors in the measurements of holdup. Holdup in the bubble flow pattern was increased up to 35%. The increase in holdup was less in the bubble-slug and curn-slug flow patterns with the deviation of about 9%. The gas velocity distribution was more uniform in the bubble flow than in the bubble-slug and the churn-slug flow patterns. Holdup in the bubble flow pattern was higher for a hydrophobic plate than for a hydrophilic plate with a maximum difference of 11%. The variation in holdup in bubble-slug and churn-slug flow patterns was within experimental errors ($<4\%$).

Polypropylene with hydrophilic characteristics gave higher holdup than polyethylene, the percentage deviation in the transition being 12.5%. But the holdup for polypropylene plate was less than that of polyethylene with hydrophobic characteristics. The gas velocity distribution was more uniform for the distributor plate with hydrophobic characteristics than with hydrophilic characteristics.

Deckwer et al's (30) plot for tap water gave the transition occurring above 0.05 m/s and holdup of about 0.22. They used a glass sintered porous plate, with a pore size of 150 microns as a gas distributor. The differences with the present work may be due to the different wetting characteristics of the materials. Van Landeghen (131) had mentioned that pseudohomogenous bubbling is favorable, when the gas distributor is made of sintered material that is effectively wetted by the liquid.

Gas holdup was measured as a function of height in the column and gas velocity. In general gas holdup was higher with the porous plate than with the sieve plate. The most predominent difference was observed in the bubble flow pattern. In the bubble-slug flow pattern the differences were small.

The effect of CMC concentration on gas holdup with the sieve plate was predictable in solutions of CMC and water alone, holdup decreased with increased CMC concentration. Gas holdup for CMC solutions with IPA was unpredictable the 0.5% solutions gave higher holdup values than all of the others including the 0.25% solution. The 0.25% and 0.75% had almost identical holdup curves for the zero liquid flow case.

Gas holdup data with the porous plate revealed the two flow patterns in which the column was operated, bubble flow and bubble-slug flow. Gas holdup in the bubble flow pattern increased faster with gas velocity than in the bubble-slug pattern. See Figures 5 and 6.

The effect of IPA on gas holdup was pronounced. Gas holdup was observed to exceed 50 percent at peaks in several solutions; 0.0%, 0.25%, and 0.5% CMC. These excessive gas holdups were possibly due to foam accumulation in the column. Foam was observed in the bubble column with all of the IPA solutions. The lower concentrations of CMC resulted in higher foam production.

The effect of CMC concentration of gas holdup was to retard it. Gas holdup increased in the bubble flow pattern with increased CMC concentration. The gas velocity at maximum gas holdup in the bubble flow pattern decreased with increased CMC concentration. In the bubble-slug flow pattern the differences were substancially less however, between various CMC solutions.

The effect of liquid velocity on gas holdup was to decrease it in the bubble flow pattern, (Figures 7, and 8). There was a negligible effect on holdup in the bubble-slug flow pattern. IPA solutions showed little change in the bubble flow pattern however, peak holdup was reduced with increased liquid velocity; probably due to the expulsion of foam from the column.

Analysis of the gas holdup data revealed flow pattern transitions at for the most part the same gas velocities as the visual observations. For both CMC solutions with and without IPA a general trend was observed in the transition gas velocity and CMC concentration. For both types of solutions this trend followed;

$$V_t = A-B(\text{CMC Conc})$$

Errors arising in the determination of these transitions at the location of peak gas holdup were not well defined in most of the gas holdup data. These errors were estimated by considering the distance between adjacent data point as the range in which the peak may lie.

In general, the bubble size is smaller near the wall and has its peak approximately at R/2. For the same gas velocity the bubble size increases with CMC concentration.

However, at high CMC concentrations, the data is scattered and no specific behavior can be interpreted. Nevertheless, for a 1.00% CMC solution, mean Sauter diameter values are very close to those from Franz et al (38).

Bubble size did not vary significantly at different axial positions in the lower portion of the column. Two positions one at 62cm and another at 141cm from the distributor were tested and approximately the same bubble size was found. However, no other higher axial position was investigated although it was evident that at high throughputs coalescence

takes an important roll.

For low CMC concentrations the formation of large bubbles starts at relatively nigh superficial gas velocities. However, with highly concentrated solutions big bubbles are evolved with gas velocities as low as 1cm/s, which represents the absence of a well defined homogeneous flow.

Interfacial area is calculated over the entire gas velocity range taking into account unimodal and bimodal distributions, Figures 9 and 10 show both of them. In both cases at low gas velocities for diluted solutions the interfacial area is calculated only with homogeneous Sauter diameter because of the absence of big bubbles. Obviously, the specific interfacial area calculated using bimodal distribution is lower than the one calculated assuming unimodal distribution and the main reason is the use of a lower value for the equivalent diameter in the latter. At high superficial gas velocities interfacial area calculated using bimodal distribution is more reliable.

At low gas velocities, for all the CMC solutions excluding 2.0%, a maximum in specific interfacial area was found. This maximum is achieved at a superficial gas velocity of 1cm/s for intermediate concentrated solutions (Figures 11,12) and at relatively higher gas velocities for the more diluted solutions (Figures 9,10). This maximum diminishes with increasing CMC concentration and its variation is directly related to gas holdup variation as expected. For the lowest maximum, 1.5% solution, a fivefold gas flow is required to achieve the same interfacial area at higher throughputs (Figure 12), which demonstrates the convenience of the homogeneous flow.

The main difference in specific interfacial area between this study and Schumpe and Deckwer (114) is at low superficial gas velocities and diluted solutions, conditions in which interfacial area presents a

maximum. This difference can be explained by the fact that these investigators correlated data found with different distributors and mostly perforated plates. Thus their generalized correlation is principally for perforated plates.

Gas holdup and superficial gas velocity were correlated using the method of least squares, by the relation

$$E_G = B\ VGS^n$$

Both B and n values were determined separately for bubble, bubble-slug and churn-slug flow patterns for all the distributors. The values obtained for B and n were given in Table 1 for different porous plate distributors.

Shah et al (120) have mentioned in their review article that for bubble flow n varies from 0.7 to 1.2. The results obtained in the present work for bubble flow were similar to the above values. In bubble-slug flow pattern n varied from 0.135 to 0.529, and in churn-slug flow n varied from 0.392 to 0.672. Holdup data was calculated from the proposed correlations in bubble, bubble-slug and churn-slug flow patterns and was compared with the experimental data. Data obtained from the proposed correlations was in agreement with the experimental data. Effect of gas distributor on holdup was also studied from theoretical correlations. Results obtained from proposed correlations were in agreement with experimental results.

Flow pattern transitions for both CMC solutions and IPA and CMC solutions were found to be inversely related to CMC concentration and thus related to apparent viscosity. Since the shear rate in the bubble flow pattern and in the bubble to bubble-slug transition had never been determined, Nishikawa (96) determined shear rates for heterogeneous flow,

a pseudo apparent viscosity was used. This pseudo apparent viscosity was defined as:

$$\mu_{app}^{1} = KV_{Gs}^{n-1} \tag{1}$$

The transition gas velocity for aqueous CMC solutions was found to fit:

$$V_{GS} = 0.0023\mu'^{-0.61}_{app} \tag{2}$$

The transition superficial gas velocity could then be determined by inserting equation 1 into 2 and rearranging:

$$LnV_{GS} = - \frac{0.69LnK + 6.075}{0.69n + 0.31} \tag{3}$$

The transition gas velocity for CMC and IPA solutions were fitted similarly this resulted in:

$$V_{GS}(T) = 0.188\,\mu'^{-0.326}_{app} \tag{4}$$

and

$$LnV_{GS}(T) = - \frac{0.306LnK + 1.671}{0.306n + 0.694} \tag{5}$$

The calculated and observed transition gas velocities were plotted in Figure 13.

Equations 3 and 5 indicate that the transition from bubble to bubble-slug flow is dependent on the rheological properties of the liquid. Prior studies (5,6,39) for Newtonian liquids indicated the

transition to be independent of viscosity.

Gas holdup data for both aqueous CMC solutions and CMC and IPA solutions were fitted to equations of the form:

$$E_G = \frac{\alpha}{\beta + K} V_{GS}^{(c-n)\gamma}$$

For aqueous CMC solutions holdup data in the bubble flow pattern for the porous plate distributor were correlated. The resulting equation was;

$$E_G = \frac{0.0694}{0.0583 + K} V_{GS}^{2.8(n-0.761)} \qquad (6)$$

The standard deviation of the differences for this equation was 0.015.

This correlation is limited to the bubble flow pattern. The maximum gas velocity in this flow pattern can be determined using equation 3.

Gas holdup data for CMC solutions with the sieve plate distributor were fitted to:

$$E_G = \frac{0.10}{0.135 + K} V_{GS}^{0.773(1.682-n)} \qquad (7)$$

The standard deviation from this curve was found to be 0.011 (Figure 14).

There is no apparent physical explanation to the form of these equations in that the addition of a constant to k makes no physical sense. Further apparent viscosity or shear stress can not be extracted from k and the velocity term in either equation. The form of the gas velocity terms however does have physical implications. The sign on the flow index "n" is positive for the bubble flow pattern and negative for the bubble slug. This indicates a different set of forces or a different balance of forces acting on the bubbles in both patterns. In the bubble

flow pattern gas holdup is proportional to $Vgs^{2.8n}$, this indicates that holdup increases with shear stress. It is possible that increased shear stress retards bubble vibrations and oscillations thus reducing interactions with other bubbles, this combined with decreased bubble rise velocities would result in increased gas holdup up to the point where bubbles are bunched too close together and begin to interact anyway. This phenomenon was noted by Schumpe and Deckwer (114) and attributed to reduced bubble rise velocities.

Gas holdup data for IPA solutions could not be correlated to any models similar to the ones used for aqueous CMC solutions. This lack of fit may have been due to the complex nature of these solutions. It was apparent in figures 15 and 16 that there were competing effects from the CMC and IPA in solution. Gas holdup was maximized in the 0.5% CMC solution and minimized in the one percent CMC solution. This would suggest that CMC and IPA interact at the interface in some way.

Bubble diameters were measured for each fluid and gas distributor. The resulting sauter mean bubble diameters varied between 0.0008 and 0.02M. Bubble diameters did not appear to correlate with gas velocity except that they tended to stay constant. No relation was sought however, due to the excessive scatter in the data; Figures 17 and 18. This scatter was most likely due to the small sample of data obtained for large diameter bubbles. The appearence of ocassional large bubbles in photographs caused the large spikes in Figures 17 and 18. This was again the result of too small a sample and a disproportionate number of small bubbles near the column wall.

COMPARISON OF RESULTS WITH LITERATURE:

FLOW PATTERN:

Schumpe and Deckwer did not discuss flow pattern transitions and the effect of CMC concentration or rheological properties on the flow pattern transitions. They did however provide a flow map whose coordinates are gas velocity and apparent viscosity. This flow map indicated a decrease in the bubble to bubble-slug flow pattern transition with increased apparent viscosity. This agreed with the present study.

The gas velocities at peak gas holdup in the bubble flow pattern reported by Schumpe and Deckwer were plotted with the data from this study as both CMC concentrations and the gas velocity predicted by equation (3), in Figures 19 and 20. Schumpe and Deckwer's data exhibited behavior that varied from the present study in Figure 19, their velocity vs. concentration data appeared to fall on a curve while data from this study fell closer to a straight line. This was probably due to differences in rheological properties of the solutions used and the use of a different gas distributor; Schumpe and Deckwer used a sintered plate with an average pore diameter of 150mm. In Figure 20 Schumpe and Deckwer's data was plotted against gas velocities predicted with equation 3 and their viscosity data. This plot showed a closer relationship between the two sets of data, Schumpe and Deckwer's values were however higher than predicted for the most part. This was possibly due to the different gas distributors.

GAS HOLDUP:

The correlation developed for gas holdup in the bubble flow pattern, equation 6 was plotted for a 1.0% CMC solution with Schumpe and Deckwer's correlation for gas holdup in the bubble flow pattern for solution

concentration greater than 0.8%, see Figure 21. Gas holdup in the bubble flow pattern was found to be higher in this study than reported by Schumpe and Deckwer. This was probably again due to difference in the gas distributors. Insertion of "k" and "n" for Schumpe and Deckwer solutions into equation 6, predicted generally higher holdup than that observed by Schumpe and Deckwer, see Figure 20.

Equation 7 was compared with Schumpe and Deckwer's correlation for holdup using a sieve plate and Godbole et als correlation for gas holdup, also with a sieve plate, see Figure 22. All three curves showed good agreement upto a gas velocity of 0.04m/s. At velocities above 0.04m/s the curves diverged, Schumpe and Deckwer's increased faster and Godbole et als increased slower than equation 6. Godbole et als curve was much closer to equation 6.

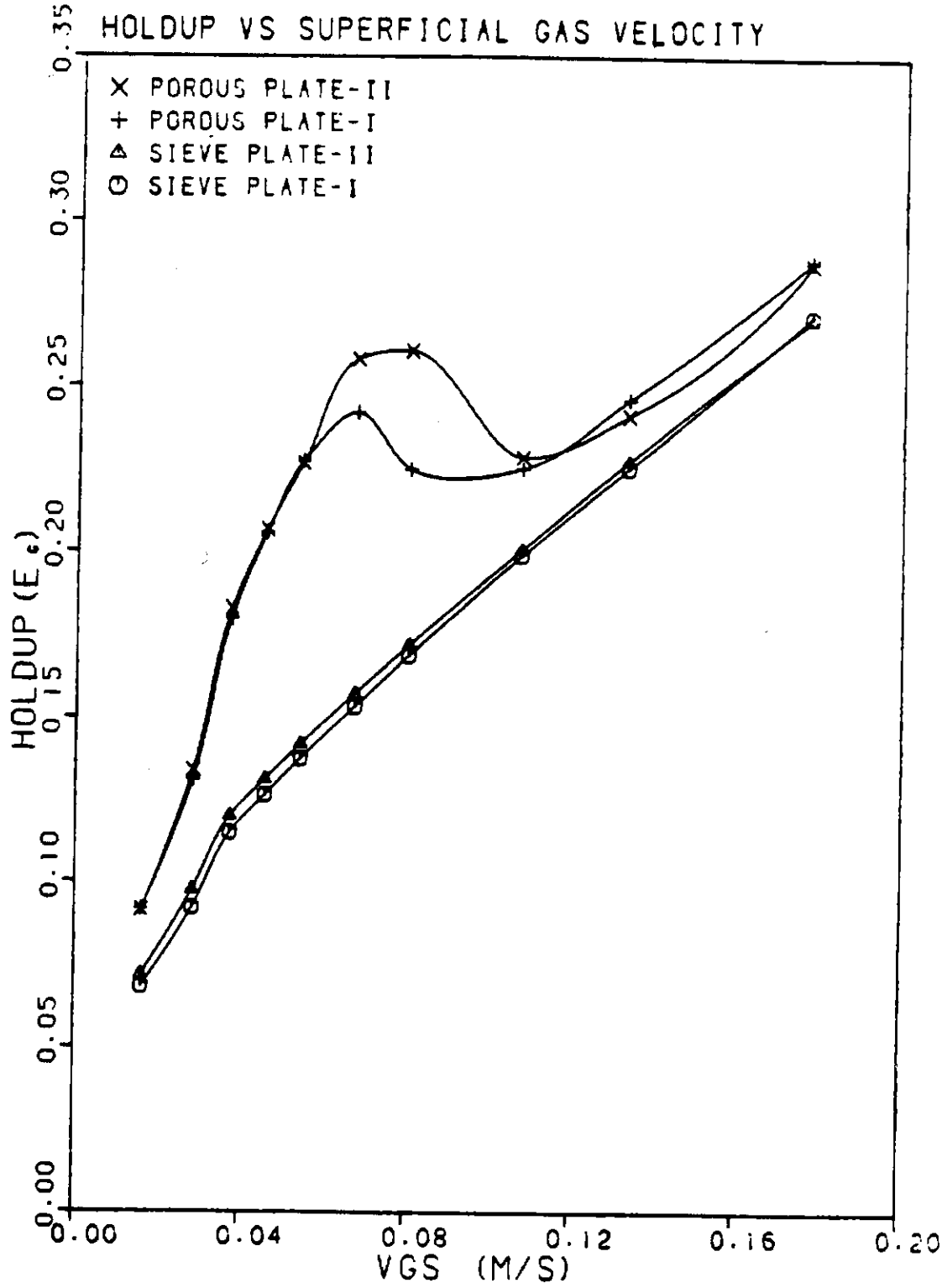

FIG. 1 GAS HOLDUP VS. SUPERFICIAL GAS VELOCITY. PRESENT WORK FOR AIR-WATER SYSTEM, 22°C, 1 ATM.

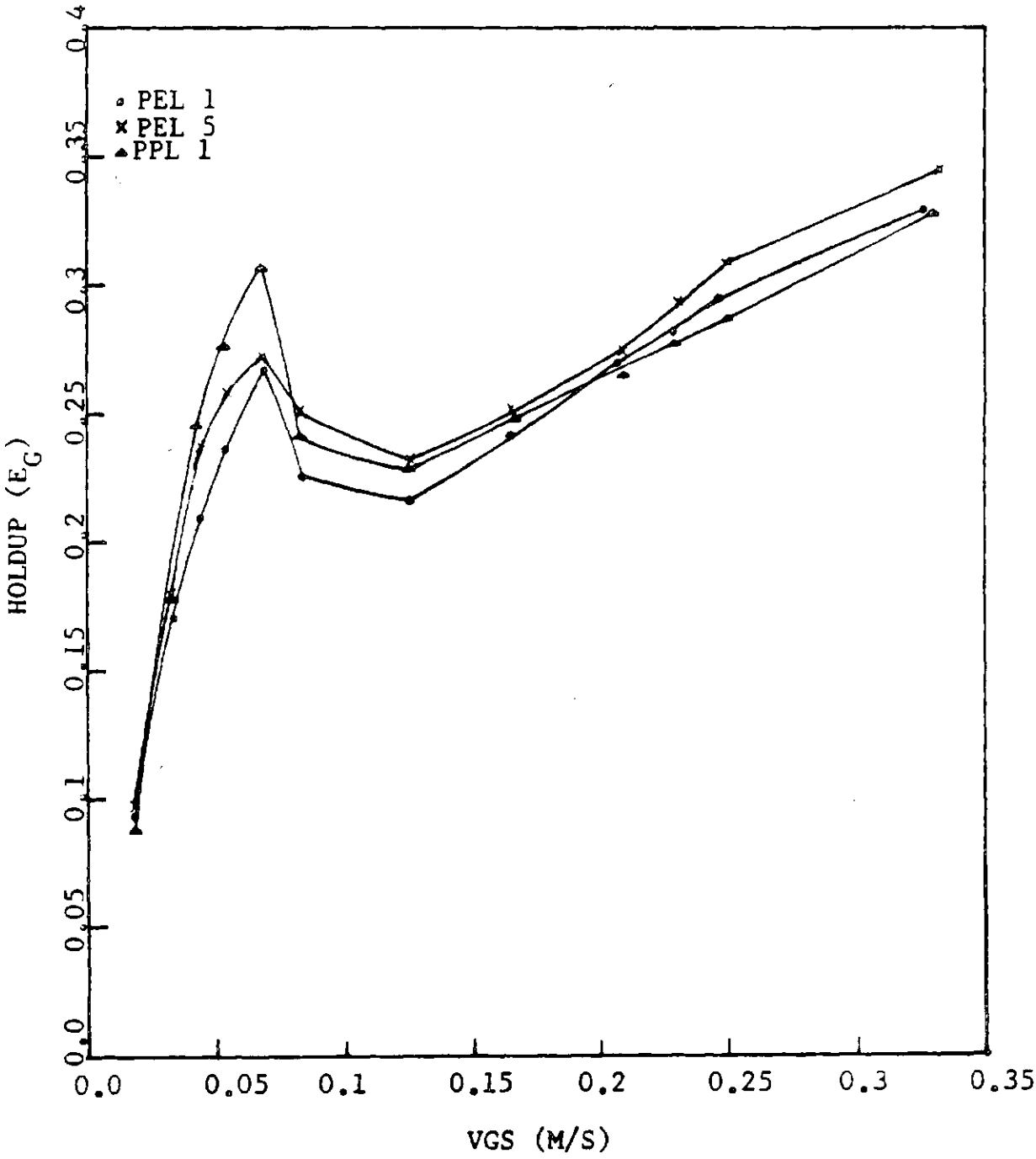

FIG. 2 EFFECT OF PORE SIZE ON GAS HOLDUP

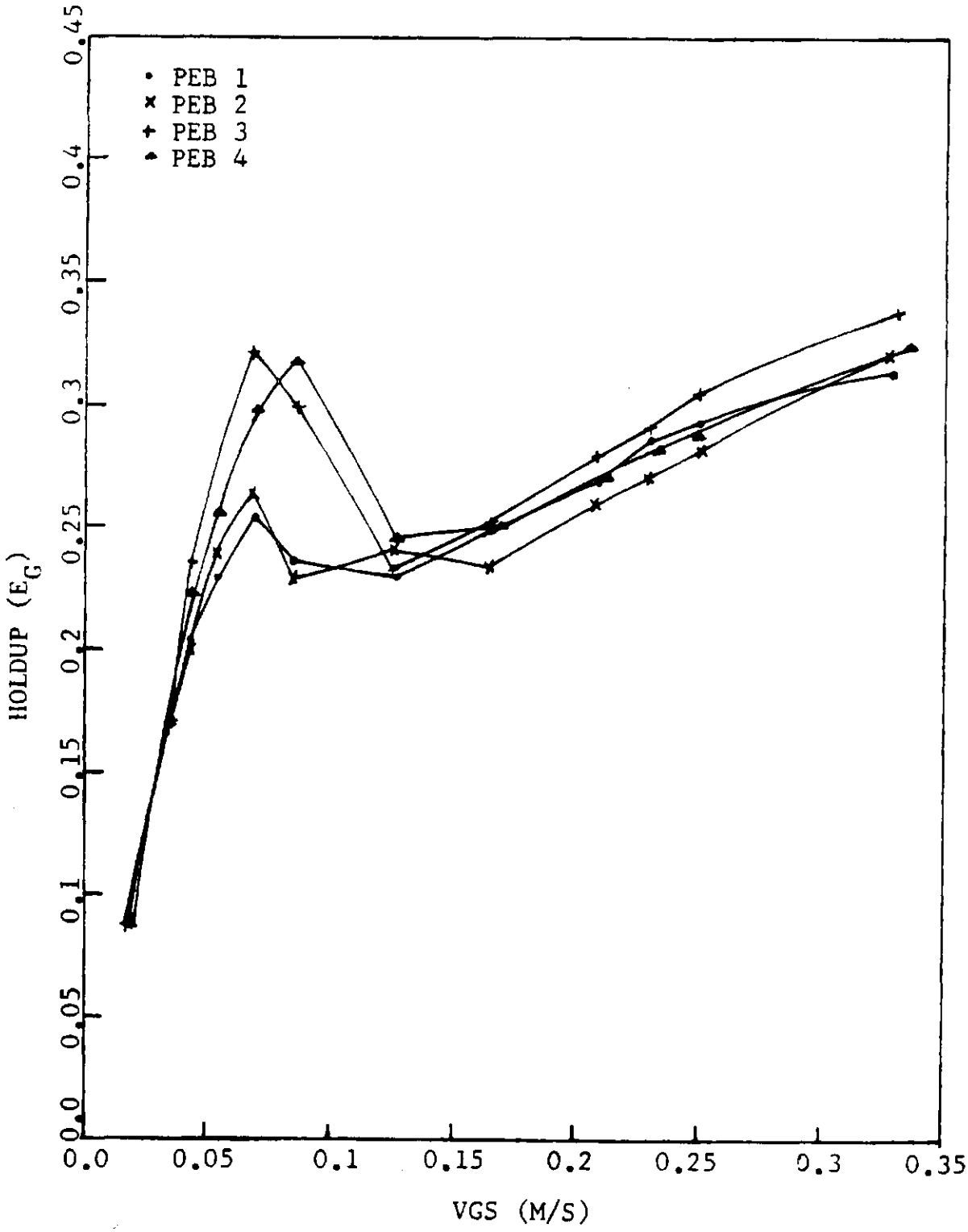

FIG. 3 EFFECT OF DISTRIBUTOR THICKNESS ON GAS HOLDUP

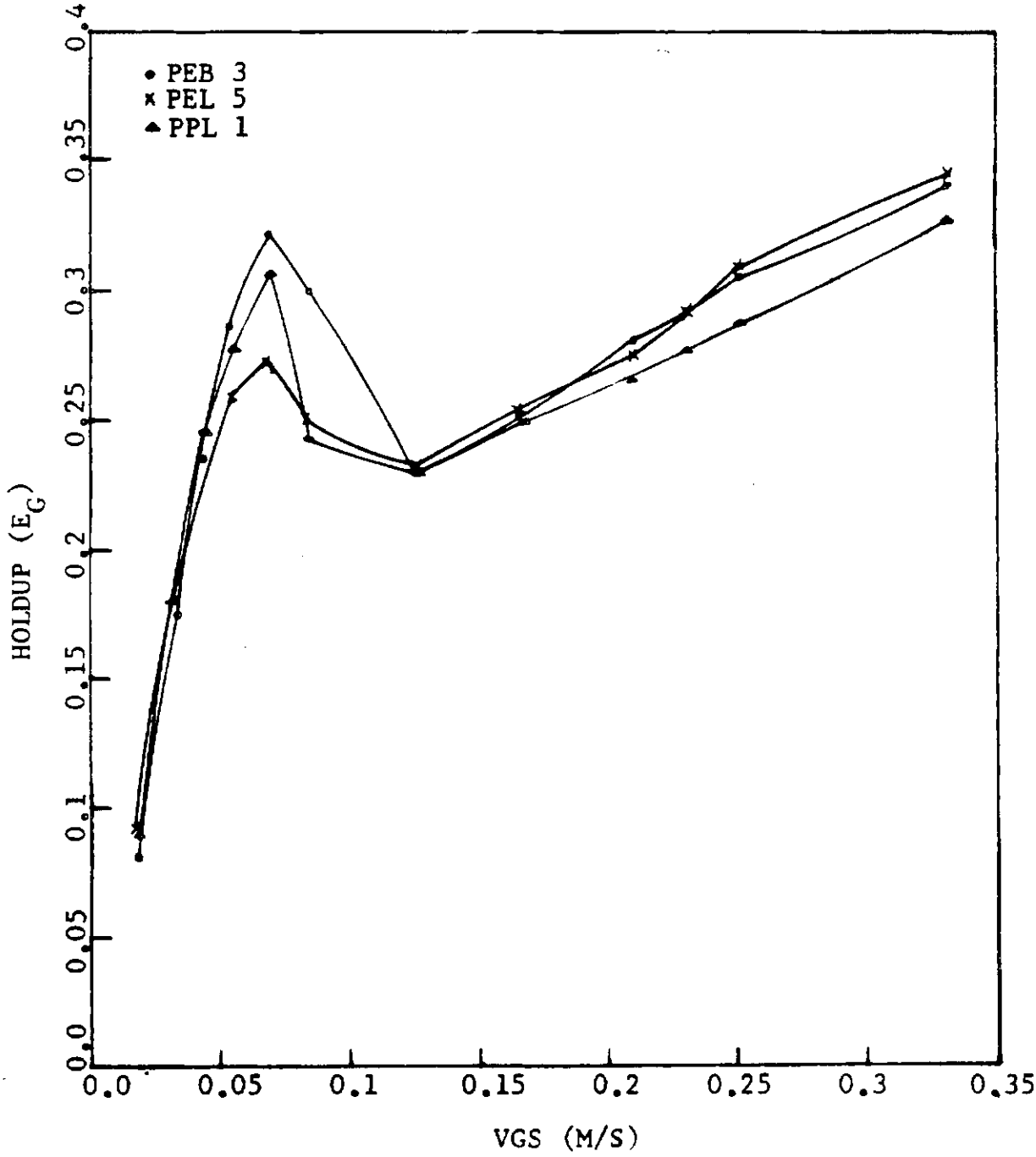

FIG. 4 EFFECT OF PLATE MATERIAL ON GAS HOLDUP

HOLDUP VS. SUPERFICIAL GAS VELOCITY

LEGEND

SYMBOL	CMC CONC.	API CONC.	LIDUID VELOCITY	DISTRIBUTOR
e	0.0	.0	0.0	POROU
▲	0.25	0.0	0.0	POROU
+	0.5	0.0	0.0	POROU
x	0.75	0.0	0.0	POROU
●	1.0	00	0.0	POROU
♦	0.75	0.0	0.0	POROU

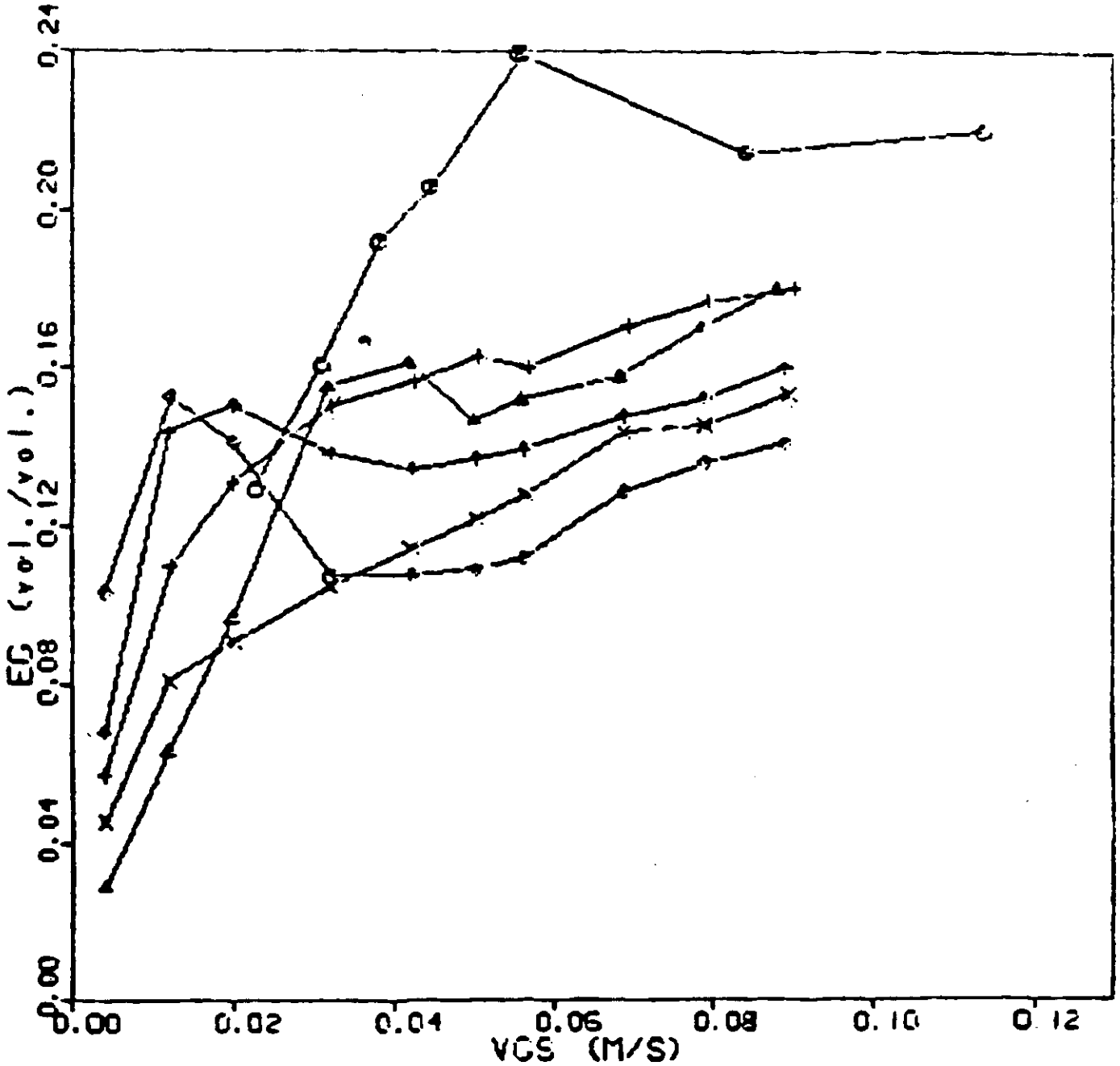

Figure 5 Effect of Porous Plate on Gas Holdup -CMC Solutions

HOLDUP VS. SUPERFICIAL GAS VELOCITY

LEGEND

SYMBOL	CMC CONC.	API CONC.	LIQUID VELOCITY	DISTRIBUTOR
o	0.5	8.0	0.012	POROU
▲	0.25	8.0	0.012	POROU
+	1.0	8.0	0.012	POROU
x	0.0	8.0	0.012	POROU

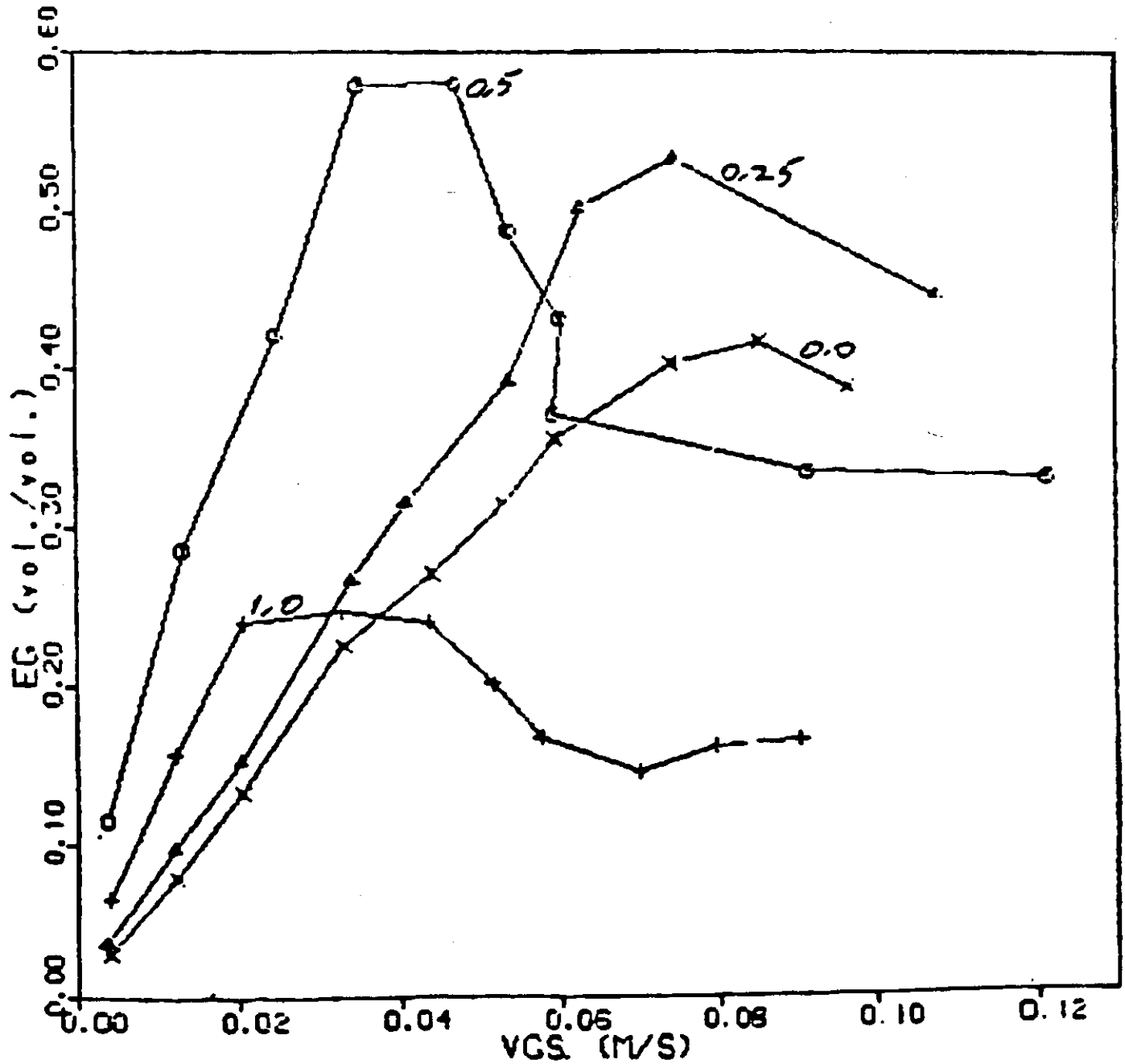

Figure 6 Effect of Porous Plate on Gas Holdup -CMC and IPA Solutions

HOLDUP VS. SUPERFICIAL GAS VELOCITY

LEGEND

SYMBOL	CMC CONC.	API CONC.	LIQUID VELOCITY	DISTRIBUTOR
○	1.0	0.0	0.0	POROU
▲	1.0	0.0	0.005	POROU
+	1.0	0.0	012	POROU
×	1.0	0.0	0.0	SIEVE
●	1.0	0.0	0.005	SIEVE
◆	1.0	0.0	0.012	SIEVE

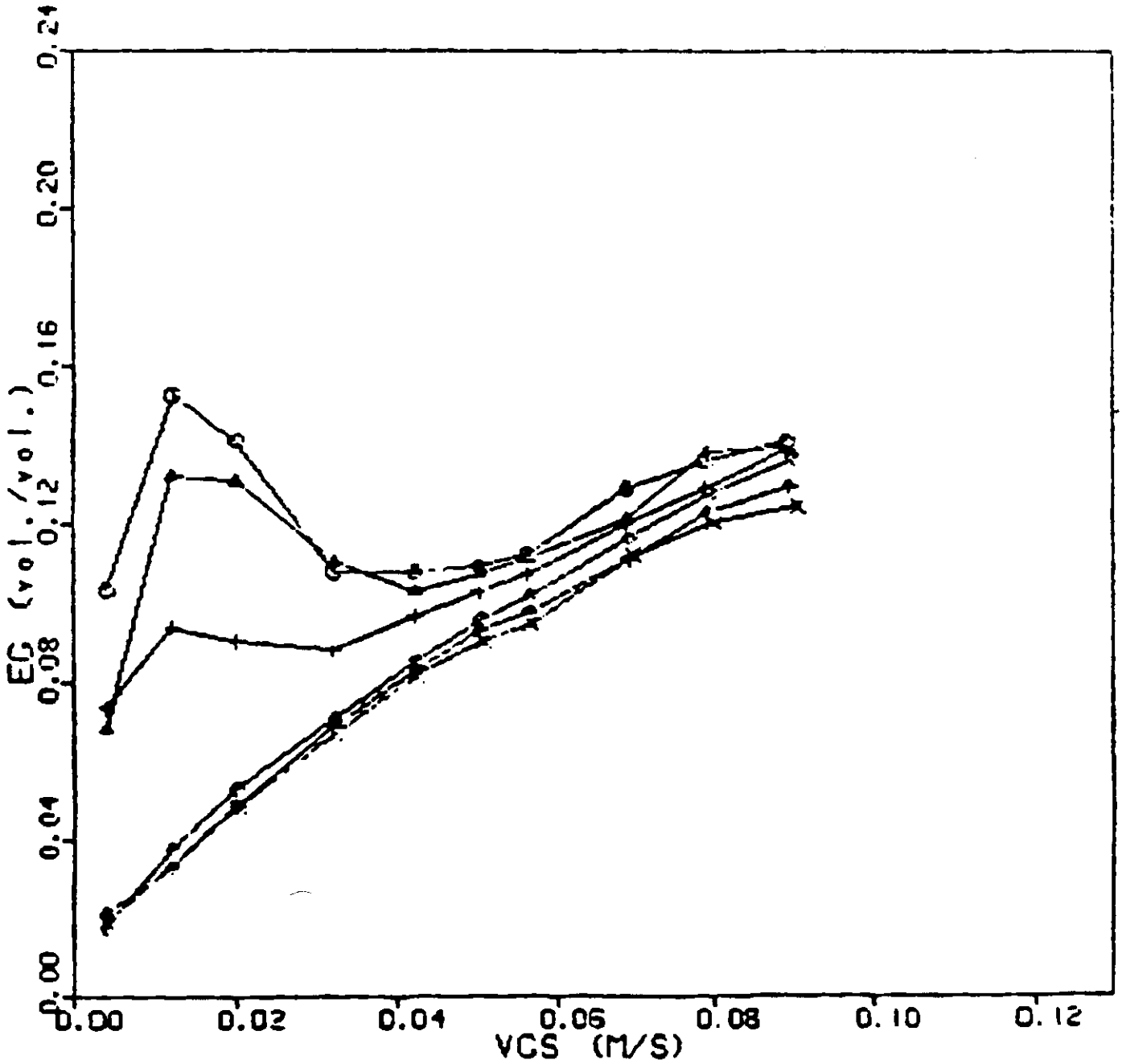

Figure 7 Effect of Liquid Velocity on Gas Holdup; 1.0% CMC

HOLDUP VS. SUPERFICIAL GAS VELOCITY

LEGEND

SYMBOL	CMC CONC.	API CONC.	LIQUID VELOCITY	DISTRIBUTOR
●	1.0	8.0	0.0	POROU
▲	1.0	8.0	0.005	POROU
+	1.0	8.0	0.012	POROU
x	1.0	8.0	0.0	SIEVE
■	1.0	8.0	0.005	SIEVE
◆	1.0	8.0	0.012	SIEVE

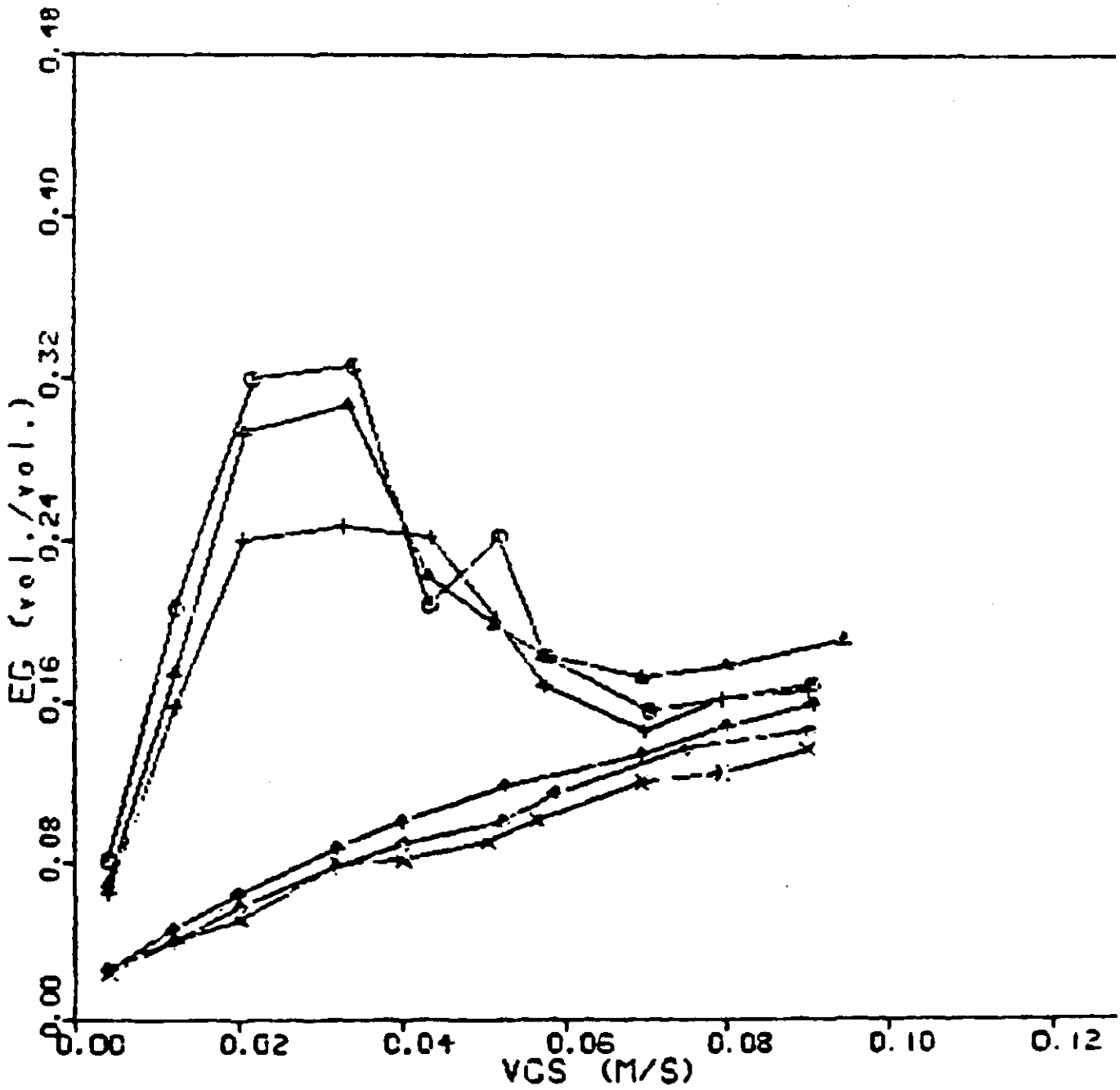

Figure 8 Effect of Liquid Velocity on Gas Holdup; 1.0% CMC, 8.0% IPA

FIGURE 9

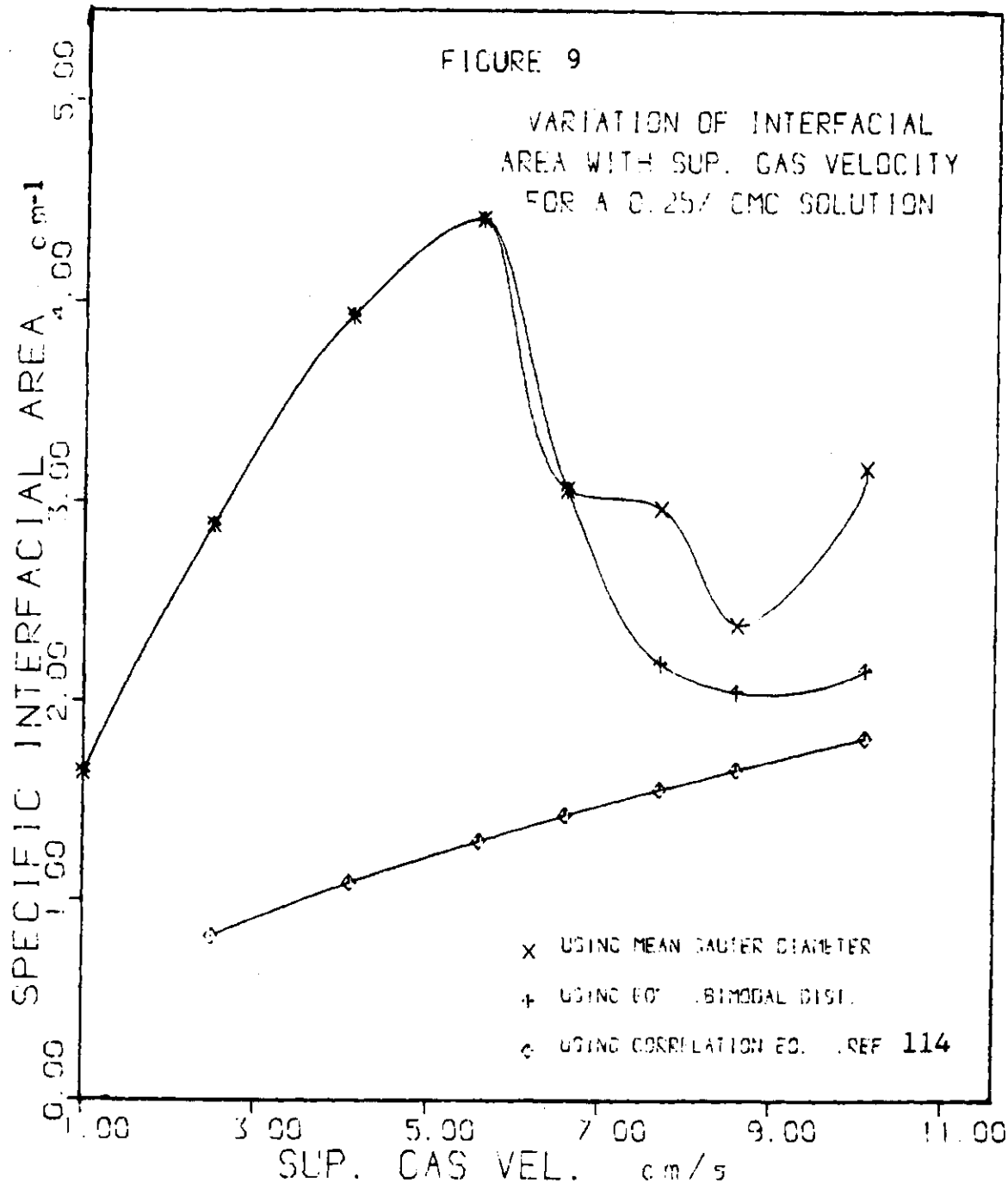
VARIATION OF INTERFACIAL AREA WITH SUP. GAS VELOCITY FOR A 0.25% CMC SOLUTION
SPECIFIC INTERFACIAL AREA cm-1
0.00
1.00
2.00
3.00
4.00
5.00
1.00
3.00
5.00
7.00
9.00
11.00
SUP. GAS VEL. cm/s
X USING MEAN SAUTER DIAMETER
+ USING BI-MODAL DIST.
◇ USING CORRELATION EQ. REF 114

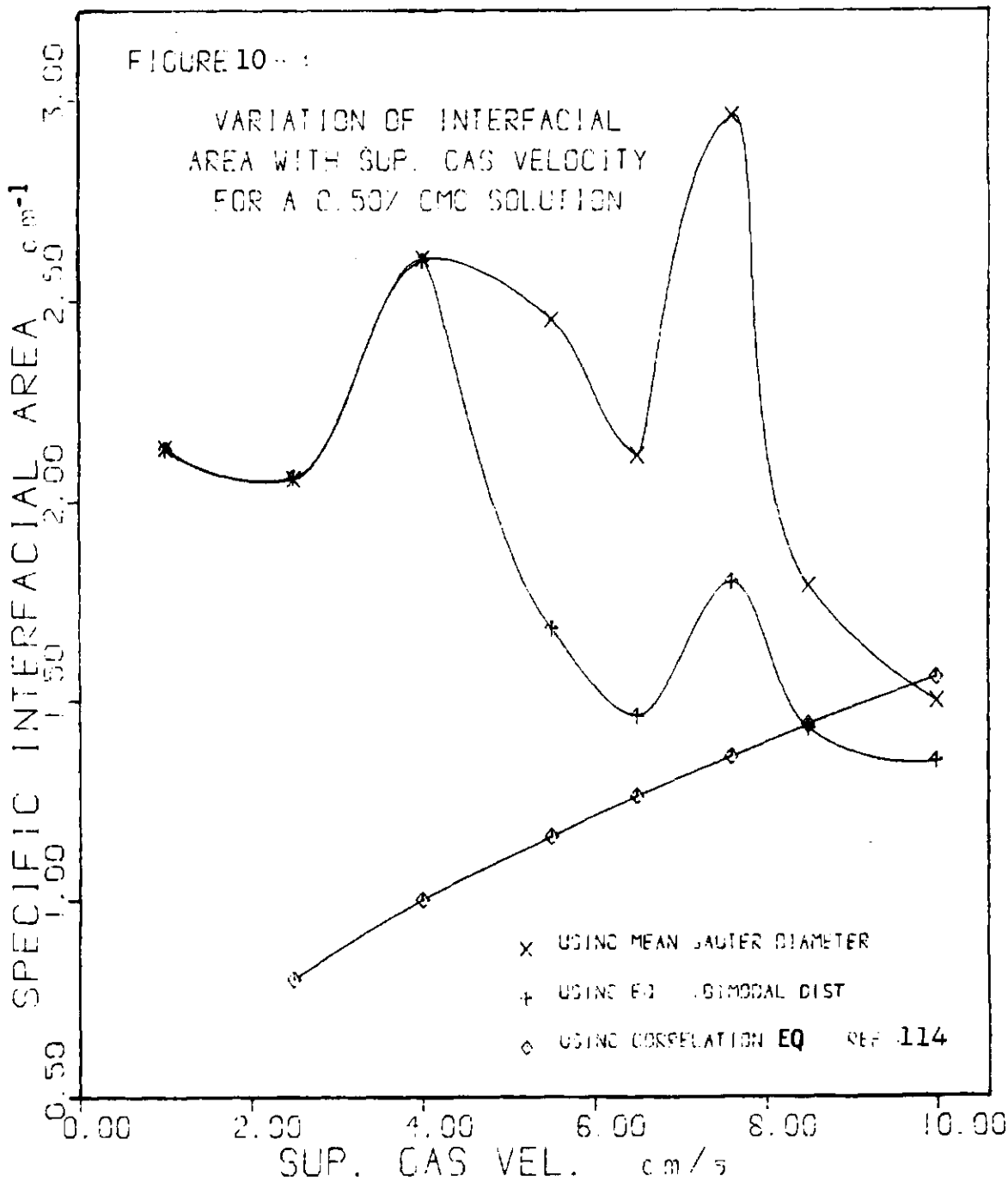
FIGURE 10 - 1
VARIATION OF INTERFACIAL AREA WITH SUP. GAS VELOCITY FOR A 0.50% CMC SOLUTION
SPECIFIC INTERFACIAL AREA cm^{-1}
0.50
1.00
1.50
2.00
2.50
3.00
0.00
2.00
4.00
6.00
8.00
10.00
SUP. GAS VEL. cm/s
X USING MEAN SAUTER DIAMETER
+ USING EQ BIMODAL DIST
◇ USING CORRELATION EQ REF 114

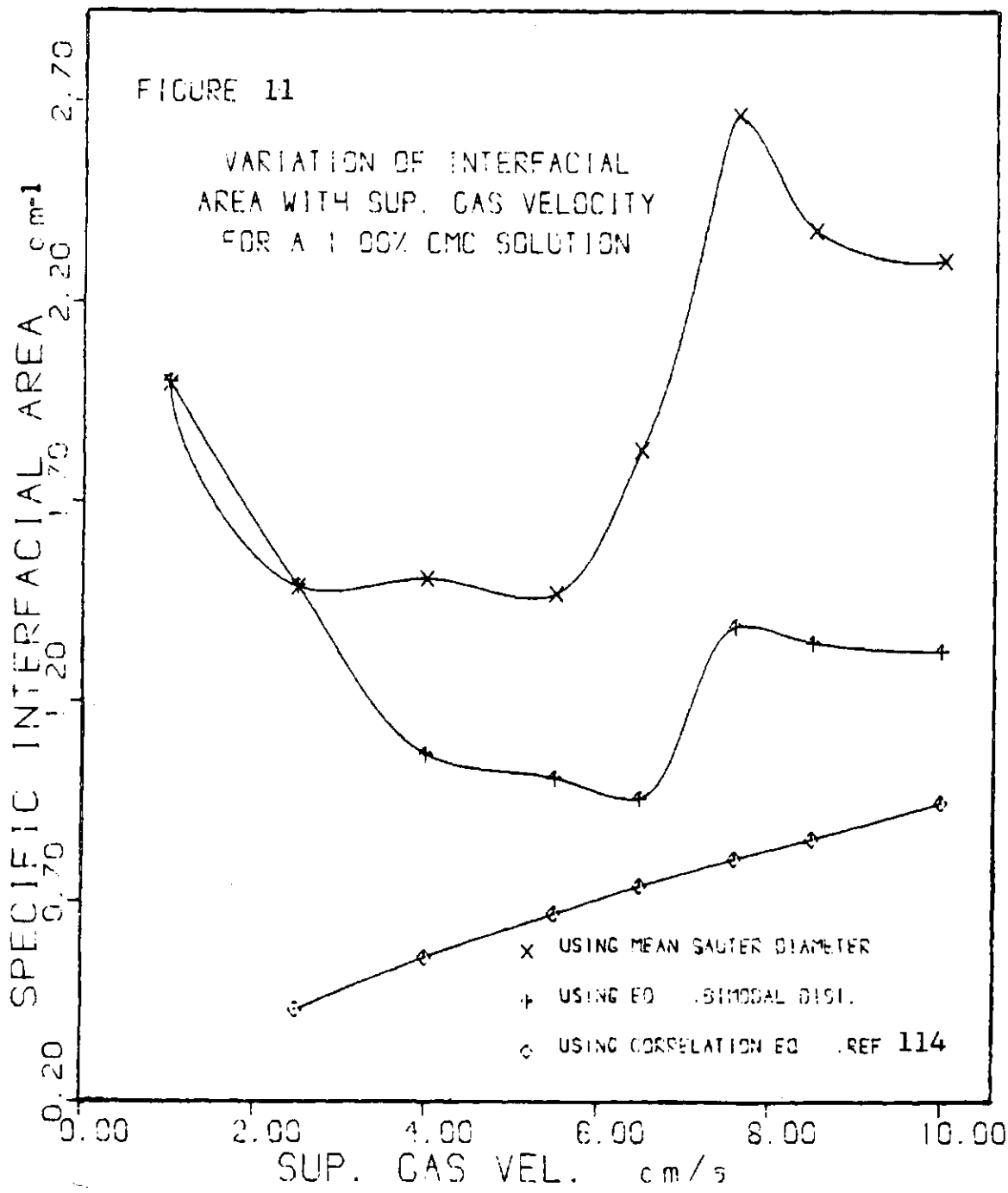
FIGURE 11
VARIATION OF INTERFACIAL AREA WITH SUP. GAS VELOCITY FOR A 1.00% CMC SOLUTION
SPECIFIC INTERFACIAL AREA cm-1
2.70
2.20
1.70
1.20
0.70
0.20
0.00
2.00
4.00
6.00
8.00
10.00
SUP. GAS VEL. cm/s
USING MEAN SAUTER DIAMETER
USING EQ. BIMODAL DIST.
USING CORRELATION EQ. REF 114

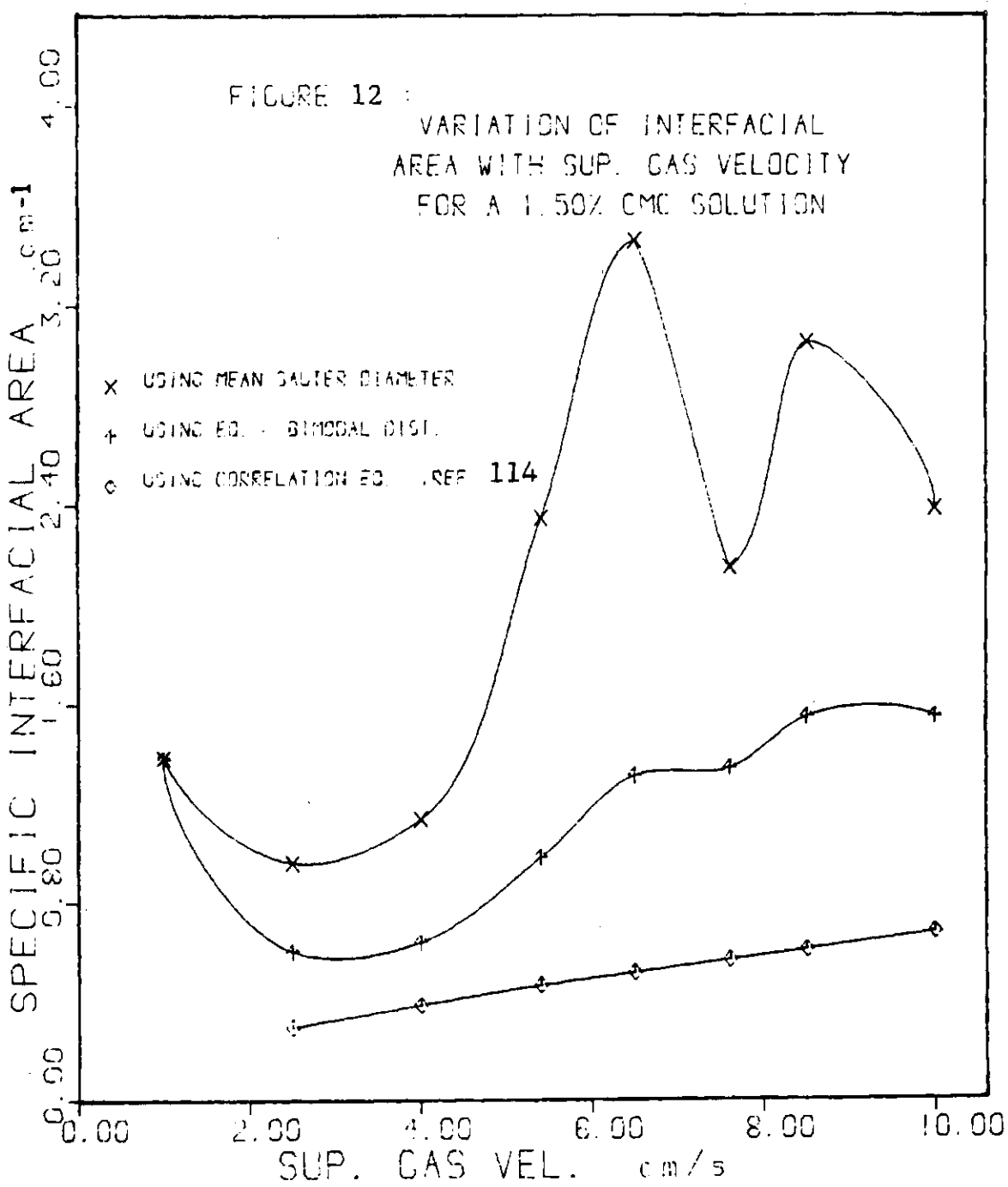
FIGURE 12 :
VARIATION OF INTERFACIAL
AREA WITH SUP. GAS VELOCITY
FOR A 1.50% CMC SOLUTION
X USING MEAN SAUTER DIAMETER
+ USING EQ. - BIMODAL DIST.
o USING CORRELATION EQ. (REF 114)
SPECIFIC INTERFACIAL AREA cm-1
0.00
0.80
1.60
2.40
3.20
4.00
0.00
2.00
4.00
6.00
8.00
10.00
SUP. GAS VEL. cm/s

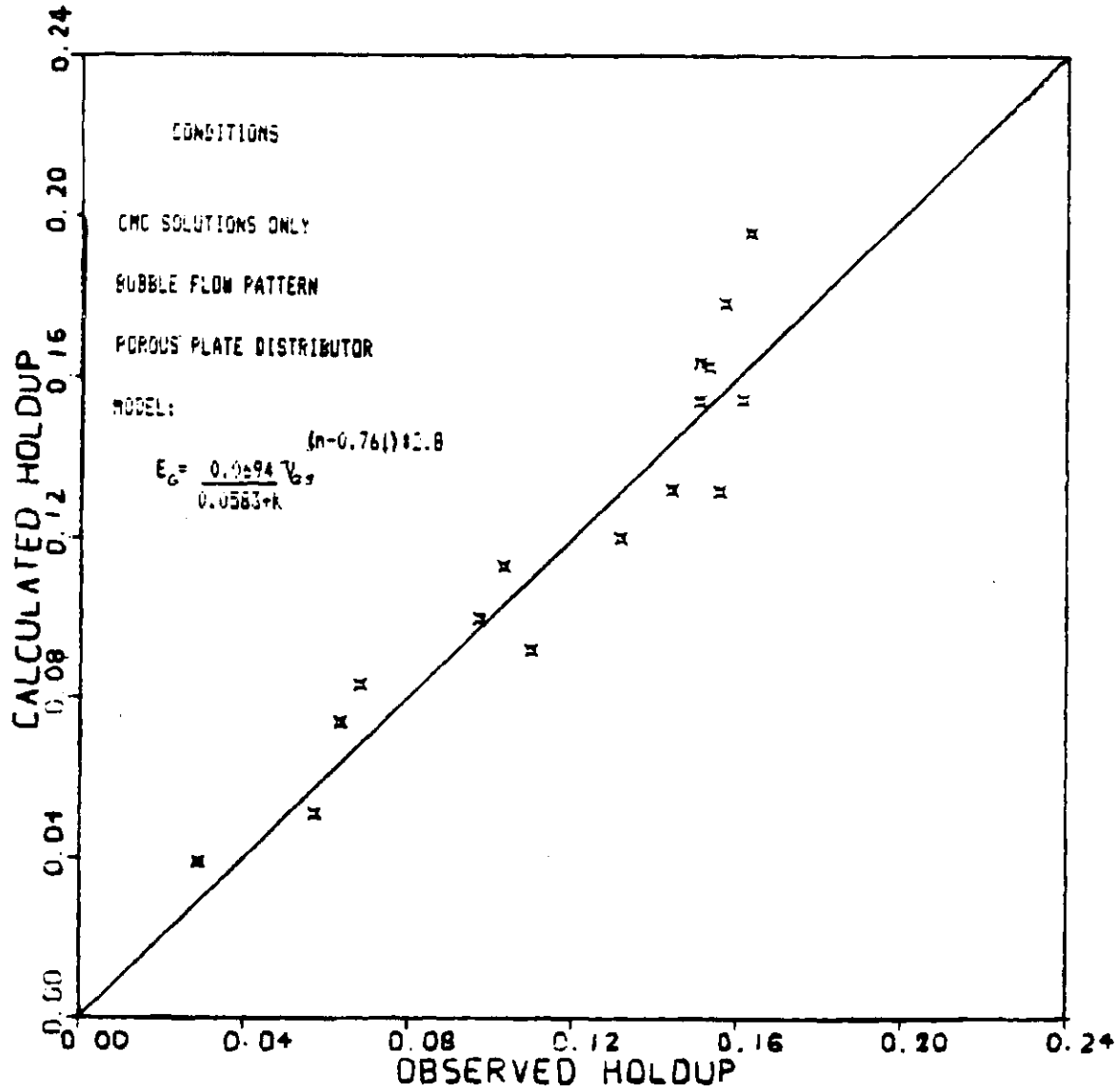

Figure 13 Parity Plot for Equation 6

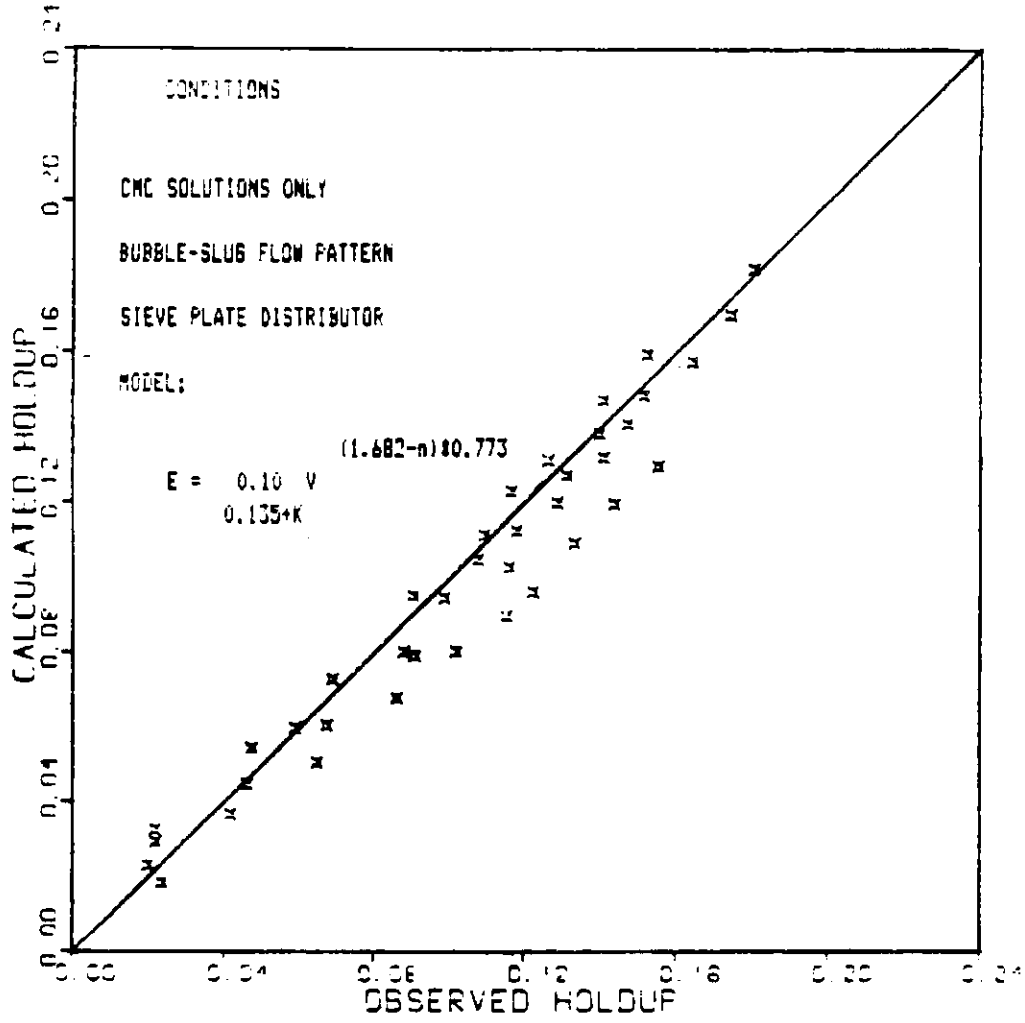

Figure 14 Parity Plot for Equation 7

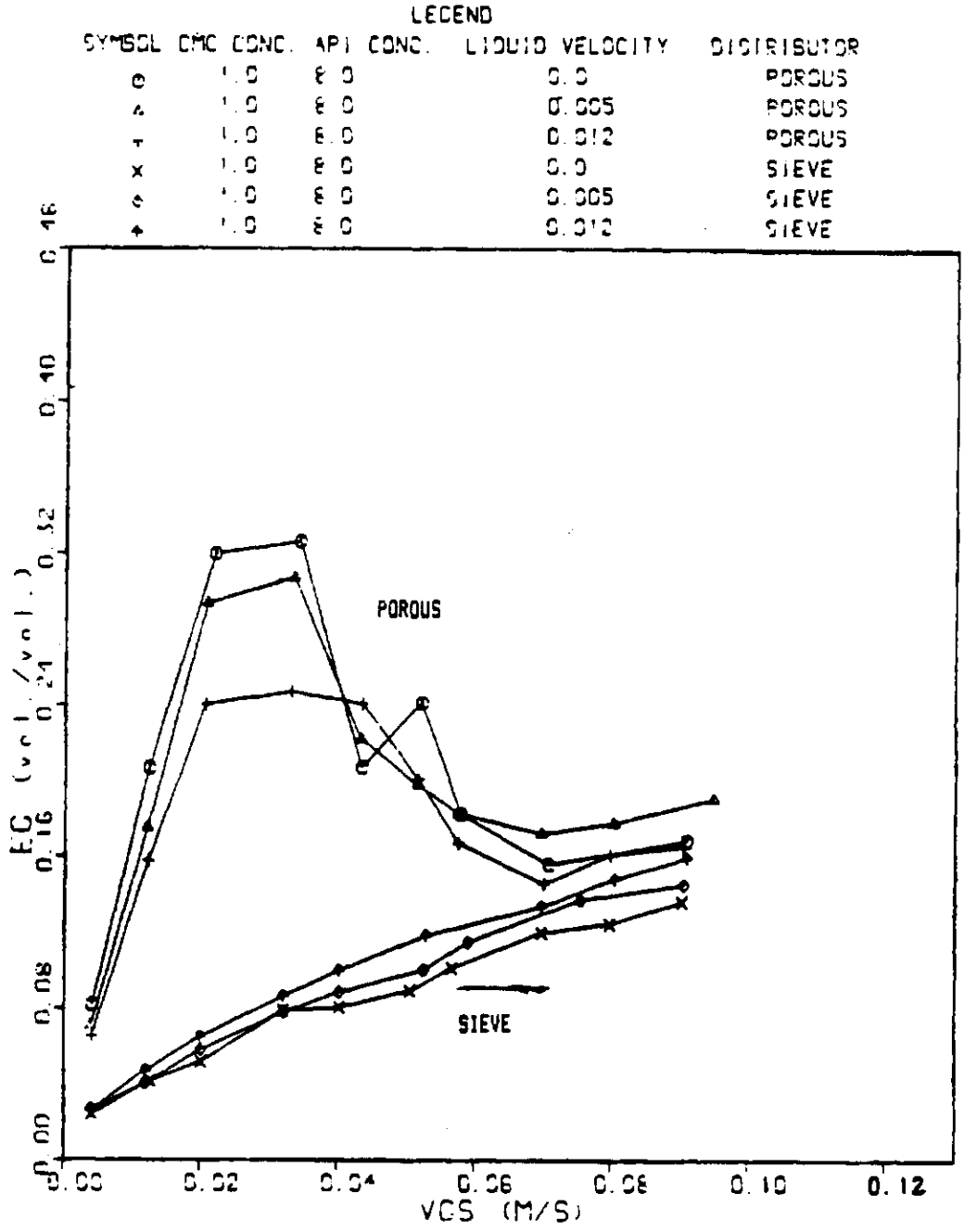

FIGURE 15 EFFECT OF LIQUID VELOCITY ON GAS HOLDUP 1.0X CMC, 0.0X IPA

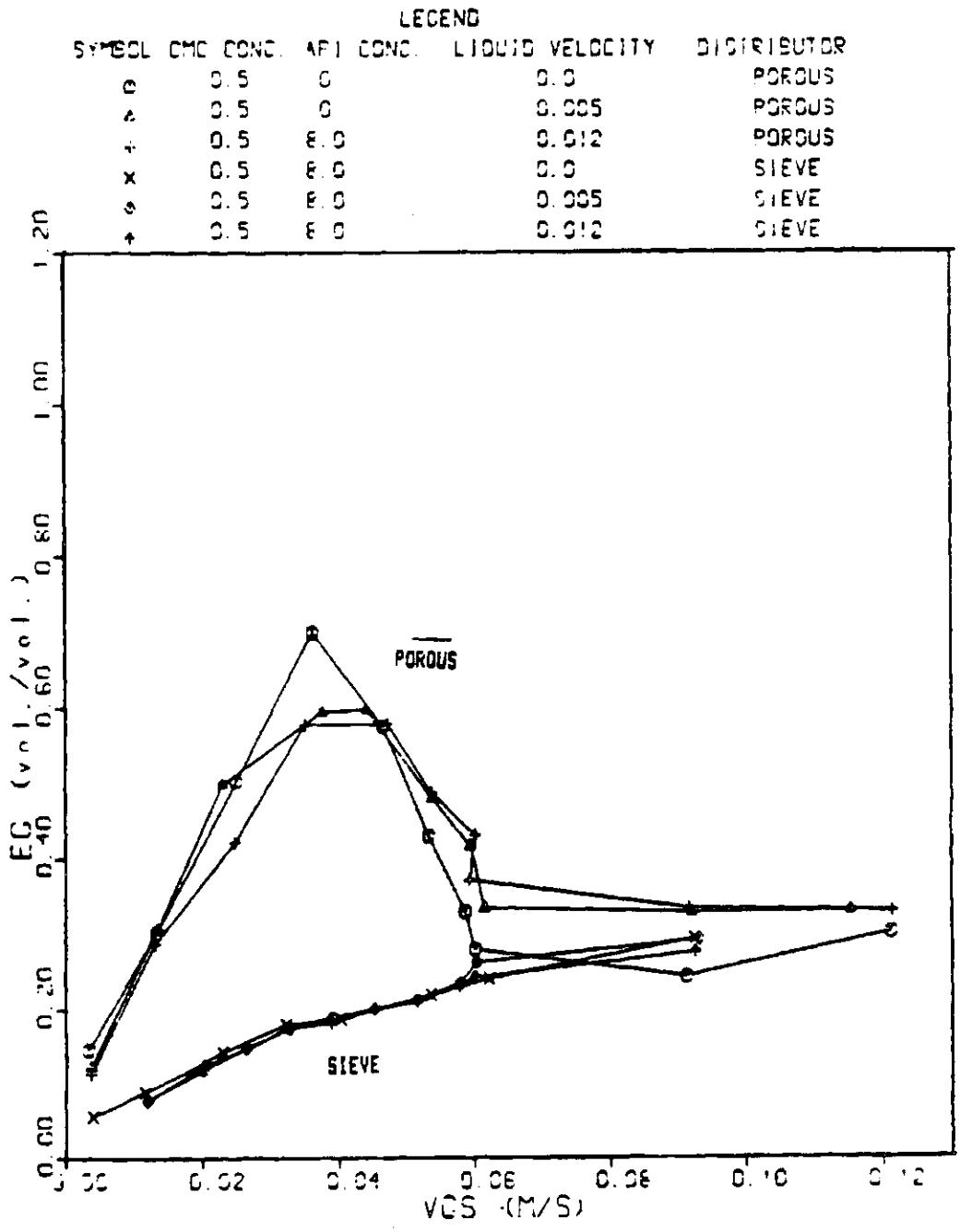

FIGURE 16 EFFECT OF LIQUID VELOCITY ON GAS HOLDUP 0.5% CMC, 8.0% IPA

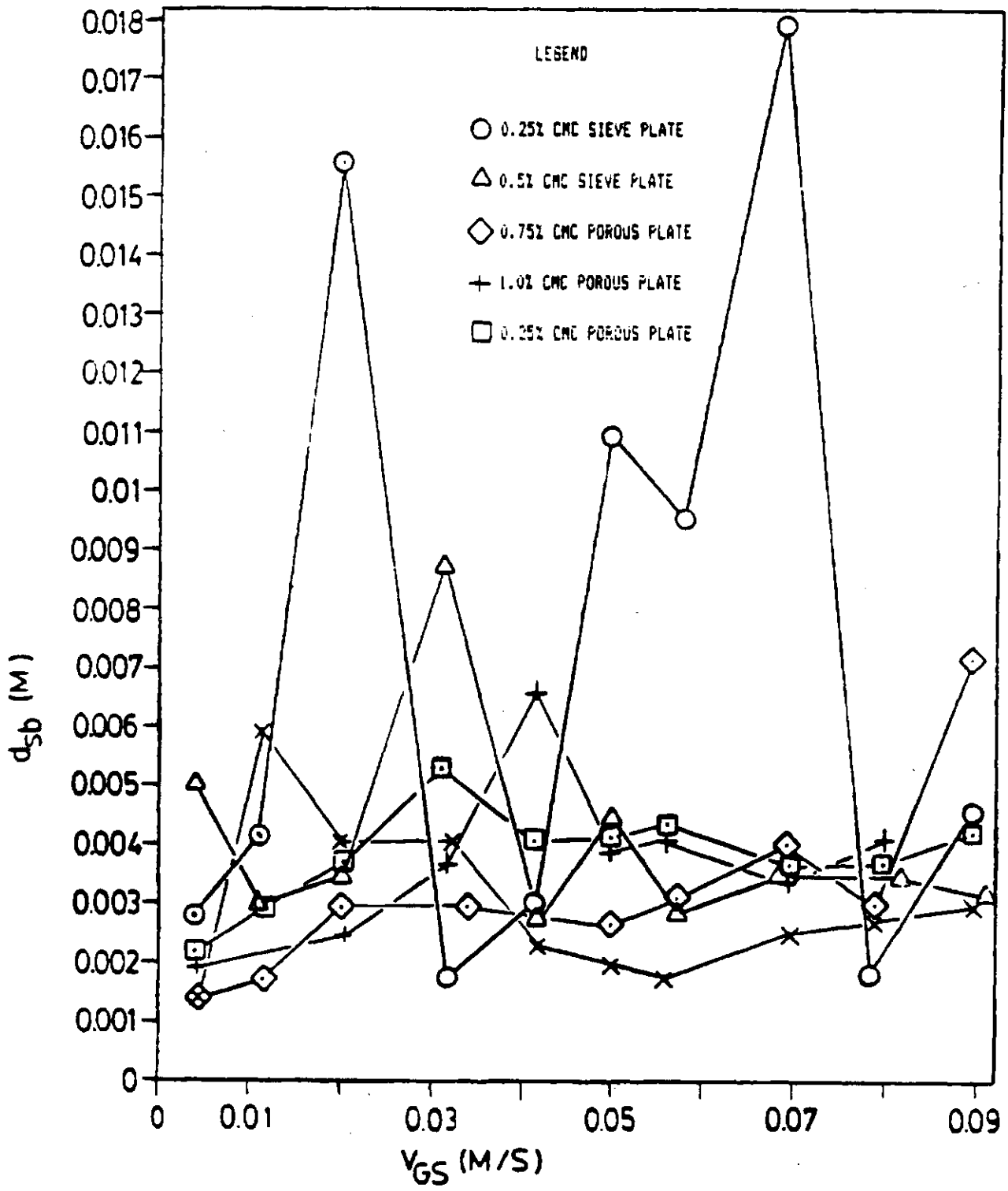

Figure 17 Variation of Bubble Sizes With Gas Velocity -CMC Solutions

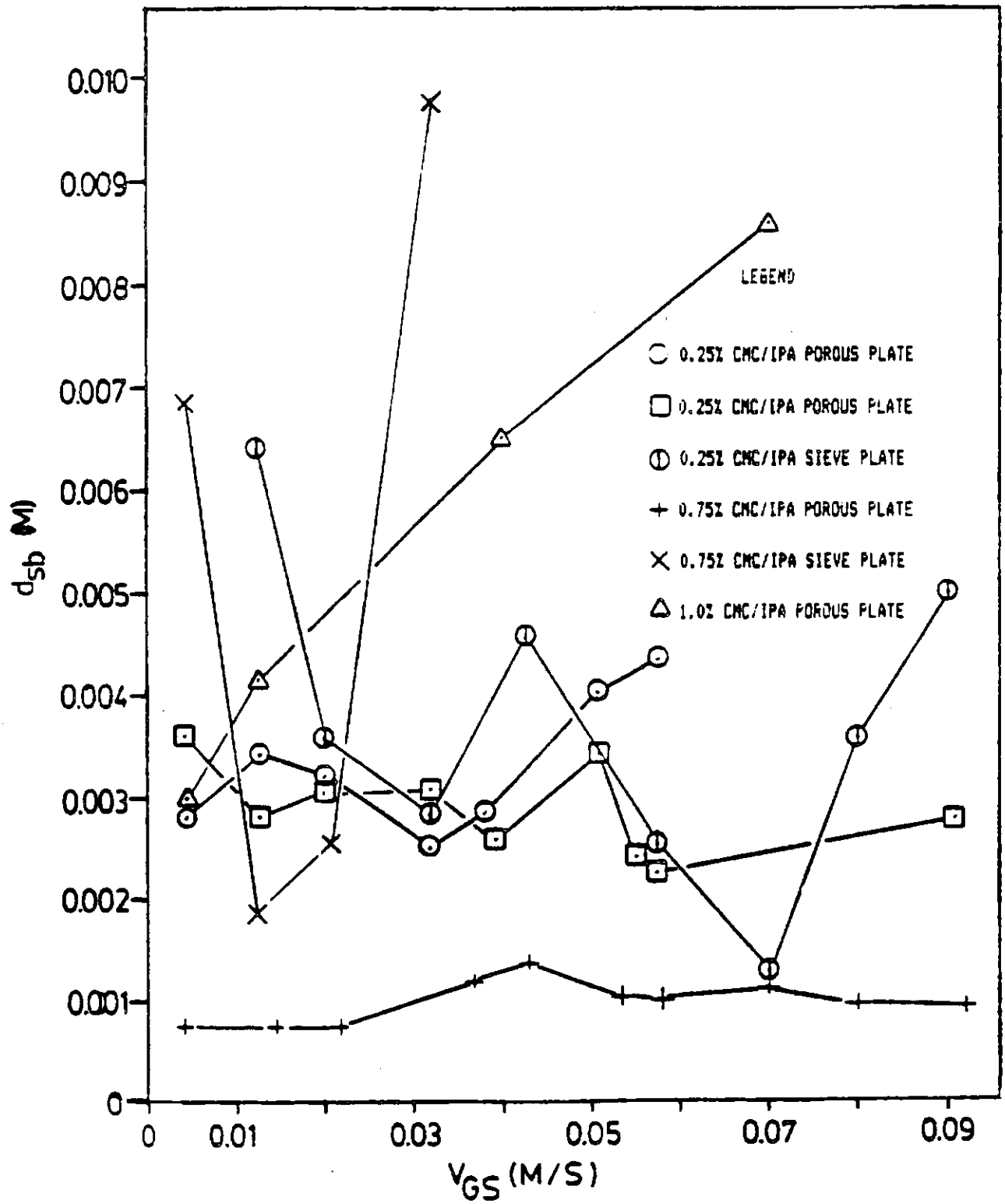

Figure 18 Variation of Bubble Sizes with Gas Velocity

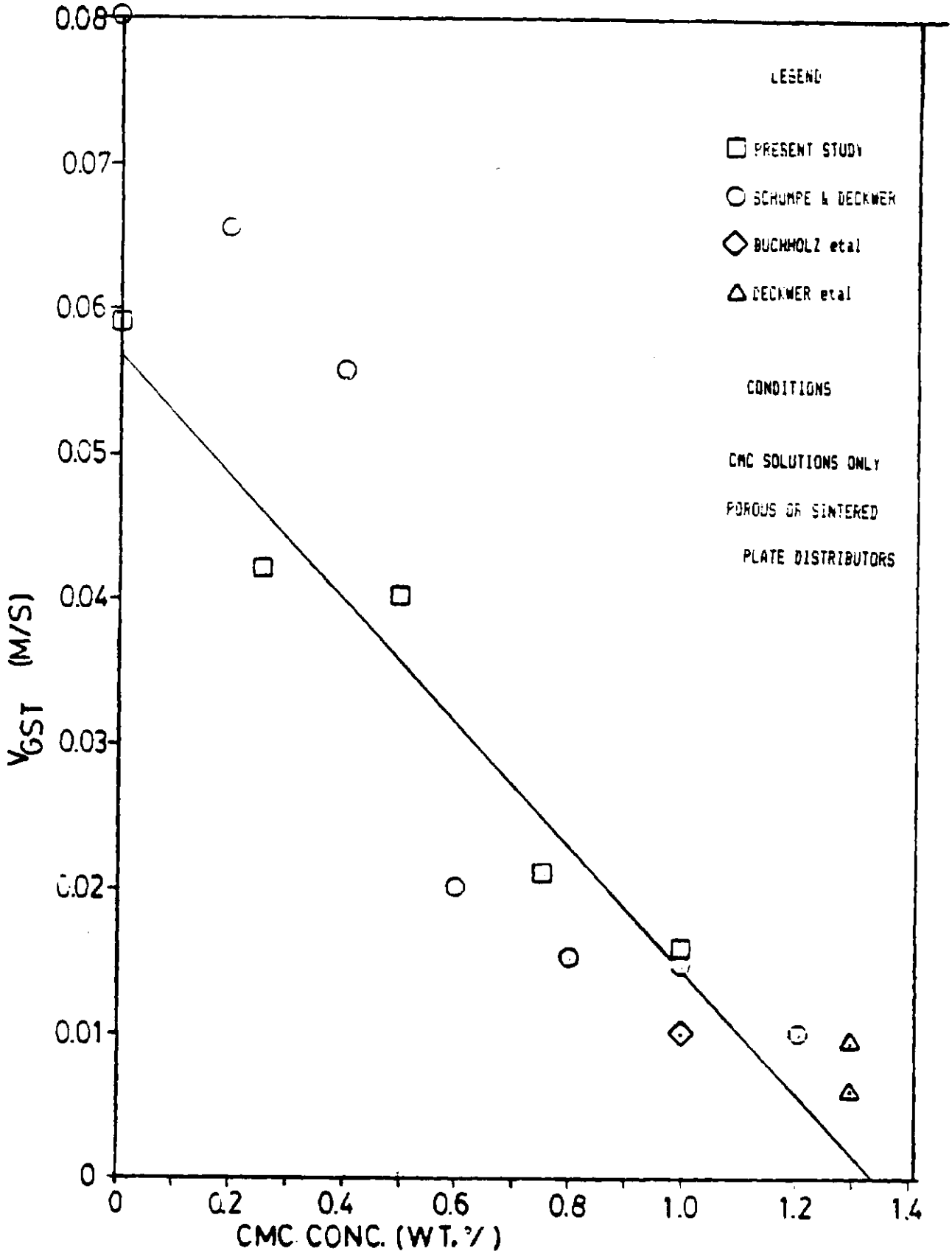

Figure 19 Comparison of Transition Gas Velocities

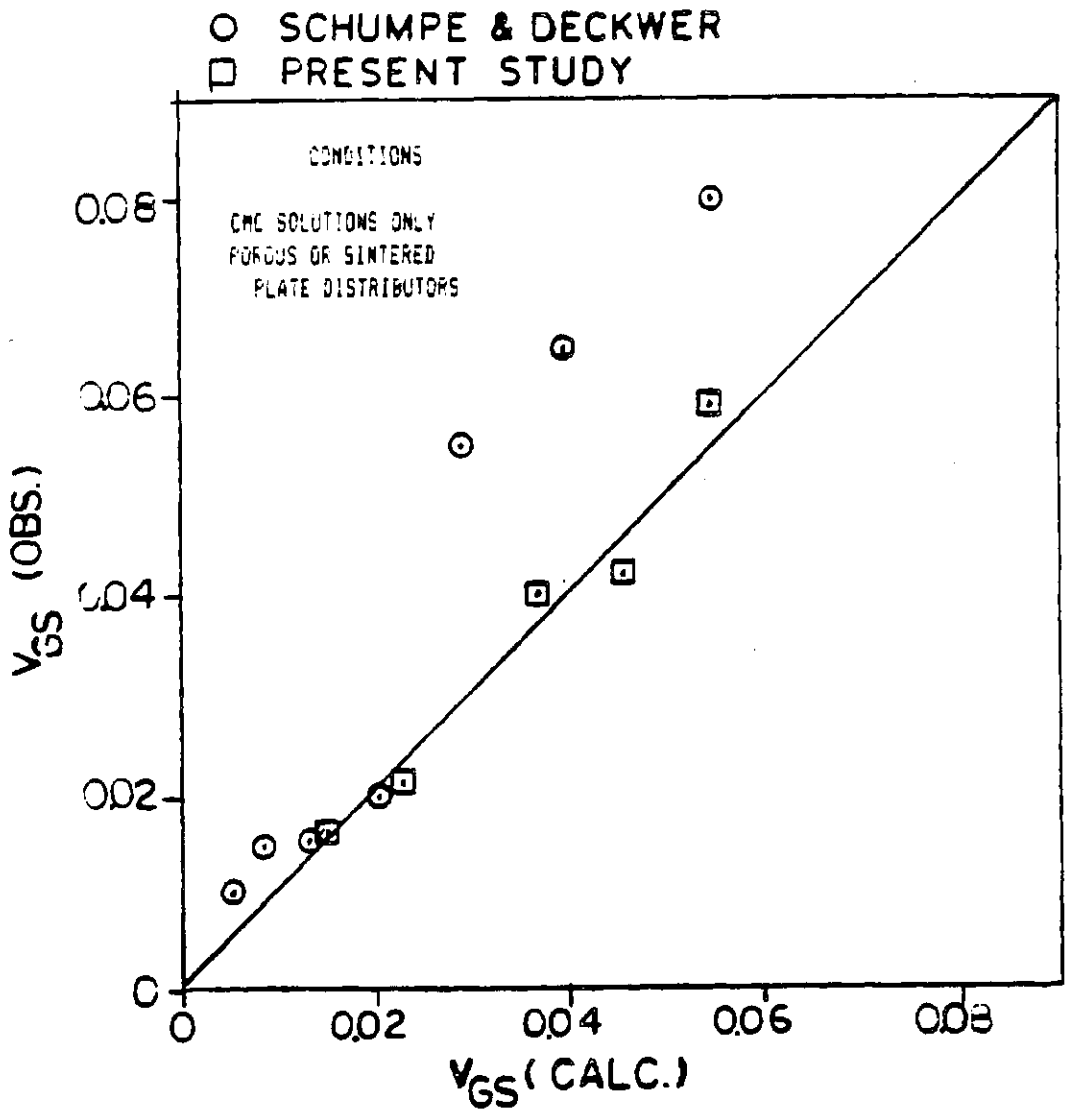

FIGURE 20 COMPARISON OF EQUATION 3 WITH LITERATURE

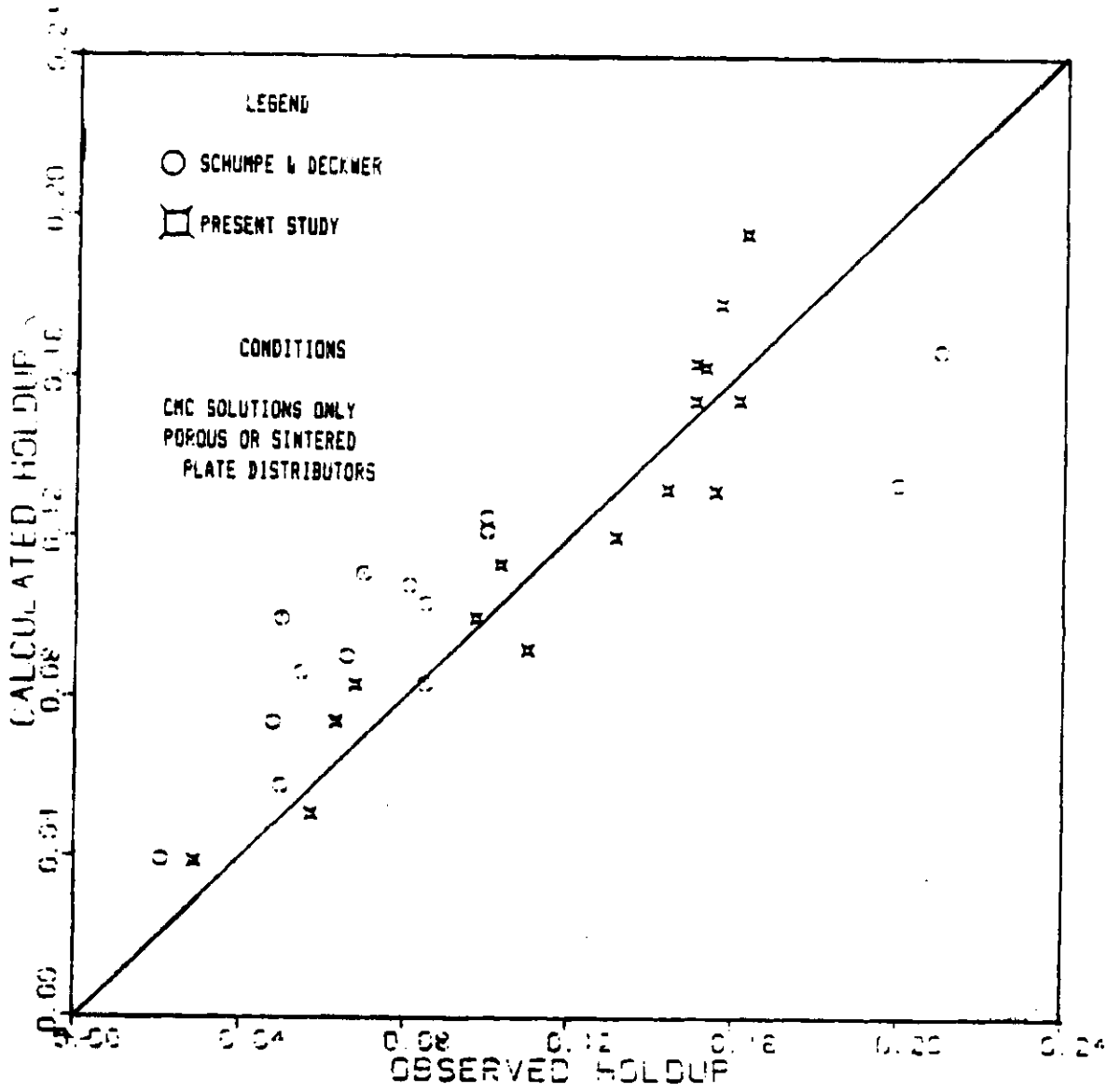

Figure 21 Comparison of Equation 6 with Literature

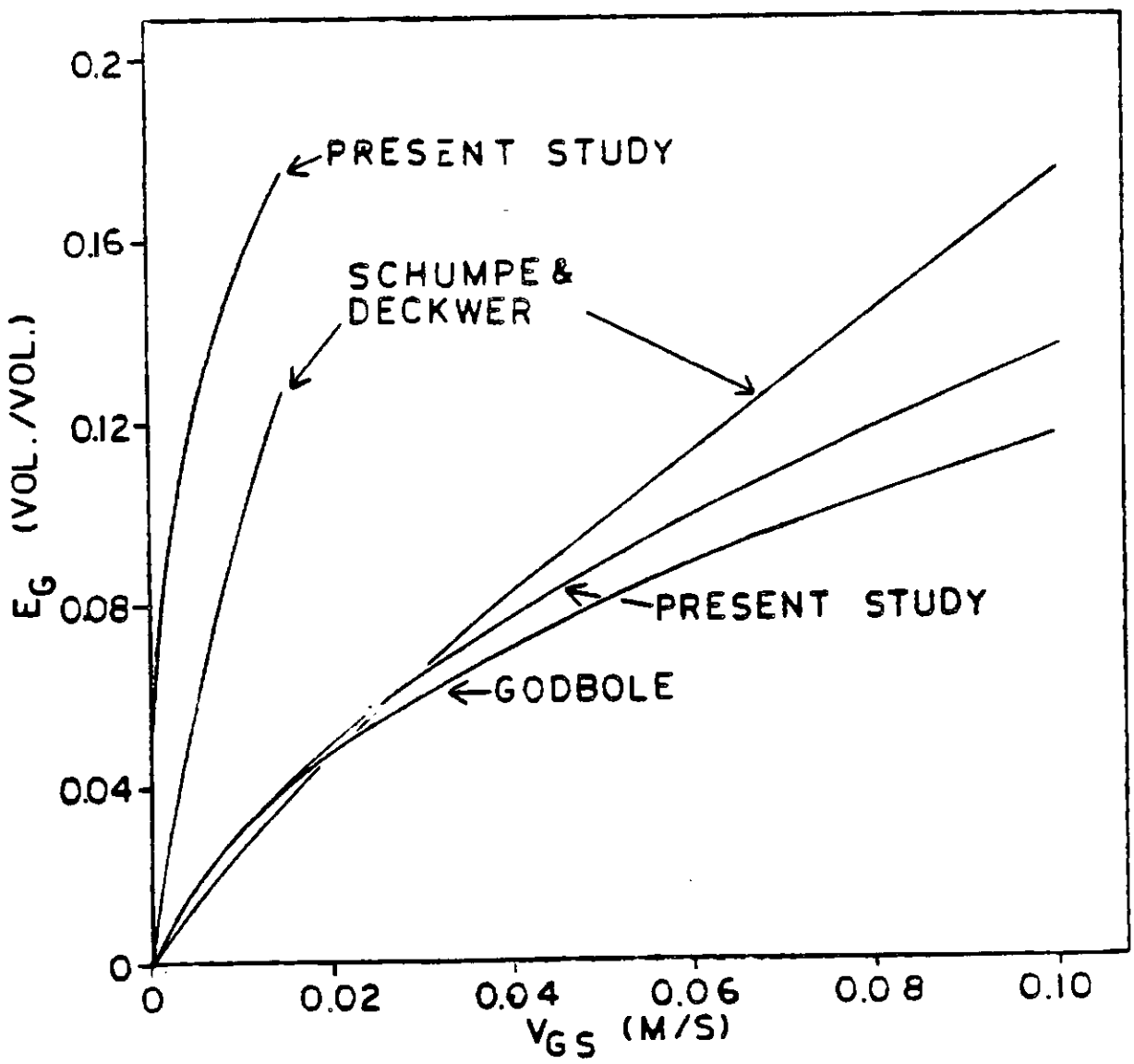

FIGURE 22 COMPARISON OF GAS HOLDUP CORRELATIONS

TABLE NO 1

HOLDUP CORRELATIONS

	BUBBLE FLOW		BUBBLE SLUG FLOW		CHURN SLUG FLOW	
PLATE	n	B	n	B	n	B
PEL 1	0.913	2.237	0.435	0.532	0.434	0.538
PEL 2	0.819	2.740	0.278	0.417	0.433	0.540
PEL 3	0.708	1.621	0.297	0.404	0.567	0.622
PEL 4	0.698	1.586	0.447	0.531	0.486	0.564
PEL 5	0.847	3.007	0.328	0.457	0.406	0.537
PEL 6	0.779	2.392	0.372	0.465	0.443	0.520
PEB 1	0.776	2.192	0.310	0.435	0.410	0.520
PEB 2	0.906	3.313	0.135	0.321	0.446	0.523
PEB 3	1.029	5.601	0.398	0.520	0.398	0.524
PEB 4	0.869	3.086	0.197	0.363	0.392	0.497
PPL 1	0.968	4.623	0.285	0.413	0.420	0.514
PPL 2	1.090	7.220	0.142	0.319	0.441	0.530
SC 1	0.840	2.534	0.173	0.293	0.542	0.575
SC 2	0.817	2.638	0.299	0.388	0.484	0.563
PP	0.772	1.944	0.355	0.436	0.565	0.628
AO 1	0.703	1.399	0.355	0.435	0.486	0.562
AO 3	0.667	1.423	0.356	0.434	0.672	0.723
SE	0.529	0.601	0.529	0.601	0.529	0.601
KAMAT	0.696	1.700	0.487	0.665		